Chair of Statistics · School of Business and Economics · Humboldt-Universität zu Berlin

Elastic Full Procrustes Means for Sparse and Irregular Planar Curves

Masters Thesis

in partial fulfillment of the requirements for the degree

M.Sc. Statistics

Manuel Pfeuffer[1]

Berlin, 12th December, 2021

Advisors: Lisa Steyer, Almond Stöcker

1st Examiner: Prof. Dr. Sonja Greven

2nd Examiner: Prof. Dr. Nadja Klein

[1] mnl.pfeuffer@gmail.com, Matriculation number: 577668

Contents

Todo list

1. Introduction

Statistical Shape Analysis (see e.g. Dryden and Mardia 2016) is the branch of statistics concerned with modelling geometrical information. Such information might come in the form of outlines of bones or organs in a medical image, traced points along a handwritten digit, or data on the folding structure of a protein. This data is commonly captured using *landmarks*, which are characteristic points on the objects of interest that "match between and within populations"(Dryden and Mardia 2016, p. 3). As an example, we might geometrically compare a set of mouse vertebrae by comparing the coordinates of prominent points along the bone outlines, which are common between all mouse vertebrae. More formally, we could say that each mouse vertebra's geometrical information is then represented by a landmark configuration $X \in \mathbb{R}^{k \times d}$, which is the stacked matrix of the k d-dimensional landmark coordinates, allowing for a multivariate treatment of shape or geometrical form.

A more flexible approach might be to treat e.g. the outline of an object as a whole, represented in the form of a continous curve $\beta : [0,1] \to \mathbb{R}^d$. Landmarks have the drawback that there is no clear way of choosing which points to include in the configuration, leaving the decision up to the subjectivity of the researcher. Furthermore, using landmarks leads to an inherently discrete treatment of the available data, which means modes of variation that lie in between landmarks may not be picked up by the analysis. By using curves, the analysis is not restricted to a fixed set of k discrete points, but instead uses all the available information. At the same time, the subjectivity in choosing the landmarks is eliminated. As each object then corresponds to one observation, this opens up a connection to the branch of statistics concerned with observations that are whole functions: Functional Data Analysis (see e.g. Ramsay and Silverman 2005).

When analyzing the geometry of objects, differences in location, rotation, and size are often not of interest. Instead, the focus lies purely on their differences in *shape*, a widely adapted definition of which was established by Kendall 1977 and which might be

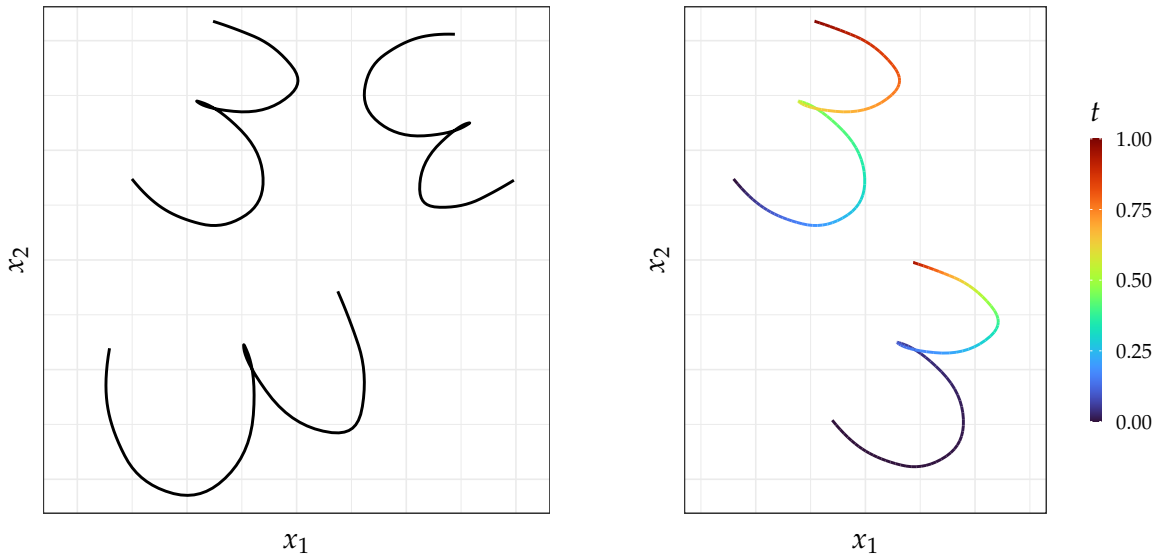

(a) The same digit with randomized rotation, scaling and translation applied three times.

(b) Original (left) and re-parameterized digit (right; $t \mapsto t^5$). Color indicates the value of the parametrization $t \in [0, 1]$ at point $\beta(t)$.

Figure 1.1.: Several representations of the same shape. Data: `digits3.dat` from the `shapes` package (Dryden 2019) for the R programming language (R Core Team 2021) with smoothing applied using methods discussed in Appendix A.2. Original dataset collected by Anderson 1997.

formulated in the following way: "[A]ll the geometrical information that remains when location, scale and rotational effects are removed from an object"(Dryden and Mardia 2016, p. 1). This is illustrated in Fig. 1.1a, where the same shape of a handwritten digit '3' is plotted in three different orientations and sizes. When considering the shape of a curve $\beta : [0, 1] \to \mathbb{R}^d$, one has to additionally take into account effects relating to the parametrization $t \in [0, 1]$. As illustrated in Fig. 1.1b, curves $\beta(t)$ and $\beta(\gamma(t))$, with some re-parametrization or *warping function* $\gamma : [0, 1] \to [0, 1]$ monotonically increasing and differentiable, have the same image and therefore represent the same shape as well.

A pre-requisite for any statistical analysis of shape is the ability to calculate a distance between and to estimate a mean from observations, in a fashion that does not depend on location, rotation, scale and/or parametrization of the input. In this thesis two established approaches to shape analysis will be combined: Firstly, the *full Procrustes distance* and *mean* are widely used for translation-, rotation-, and scaling-invariant analysis of landmark data (see e.g. Dryden and Mardia 2016, Chap. 4, 6). Secondly, Srivastava, Klassen, et al. 2011 introduced a mathematical framework for the *elastic*

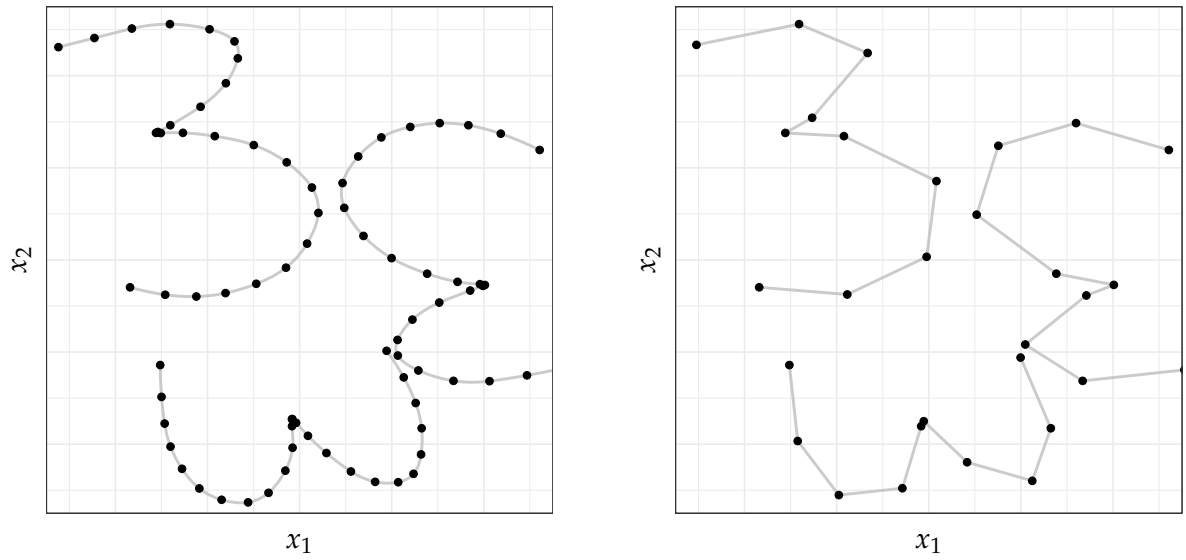

Figure 1.2.: Dense (left) and sparse (right) observations of the same three digits. Data: see Fig. 1.1, with the smooth curves sampled on a dense (left) and sparse (right) grid.

(re-parametrization invariant) shape analysis of curves, by using their square-root-velocity (SRV) representations. Taken together, both approaches allow for analyzing curves in a fashion that is invariant to all four shape-preserving transformations, leading to an *elastic full Procrustes distance* and *mean*. As the full Procrustes mean has particularly nice properties in two dimensions, when identifying $\mathbb{R}^2$ with $\mathbb{C}$ (see Dryden and Mardia 2016, Chap. 8), this thesis will be restricted to the case of planar curves.

While we are interested in modelling a (planar) object's geometrical information as a continous curve $\beta : [0, 1] \to \mathbb{R}^2$, the curve itself is usually only observed as a discrete set of points $\beta(t_1), \beta(t_2), \ldots, \beta(t_m)$. As shown on the left side of Fig. 1.2 this is no problem when the number m of observed points is high and the whole length of the curve is densly observed, as we can easily interpolate $\beta(t)$ for any $t \in [0, 1]$. However, in cases where β is only observed over a small number of points (right side) and where the density and position of observed points may even vary between different curves—a setting known as *sparse* and *irregular*—more sophisticated smoothing techniques have to be applied. While the SRV framework has been combined with a Procrustes distance before, to estimate elastic shape means that also include invariance under scaling, rotation and translation (see Srivastava, Klassen, et al. 2011), these approaches

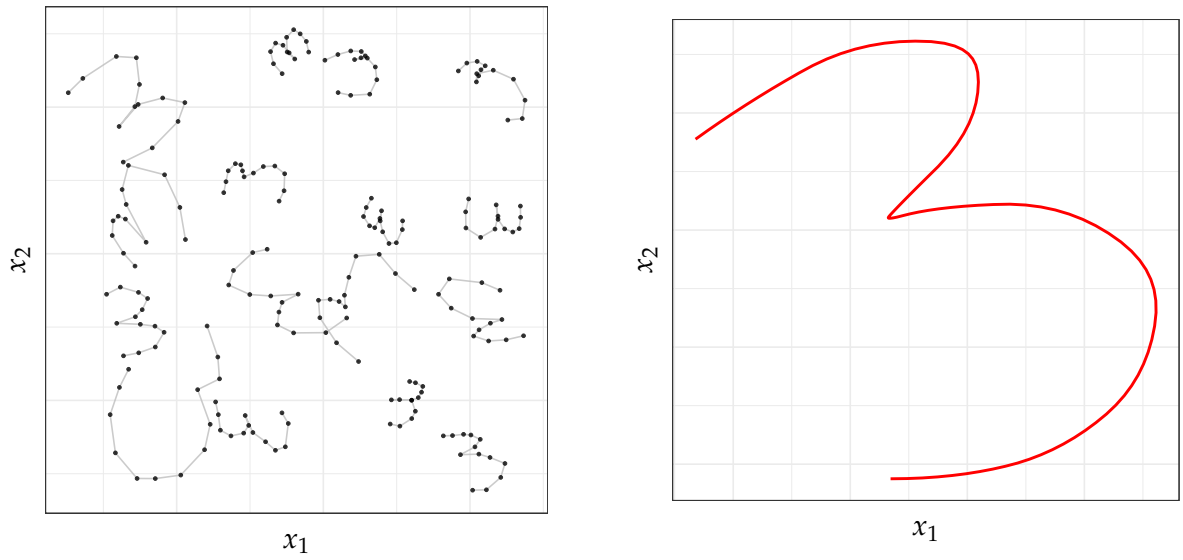

Figure 1.3.: Elastic full Procrustes mean function (right) estimated from sparse and irregular observations (left) using a 13 knot linear B-spline basis, with a 2nd order roughness penalty on SRV level. Data: Original (un-smoothed) `digits3.dat` with additional random rotation, scaling and translation applied.

have mostly focused on *Riemannian* or *geodesic* mean concepts and are not specially designed with sparse or irregular observations in mind. On the other hand, as will be shown, the estimation of the *elastic full Procrustes mean* in two dimensions is related to an eigenfunction problem over the complex covariance surface of the observed curves. This offers an advantage, as we can then make use of established smoothing techniques for the estimation of covariance surfaces in the sparse and irregular setting. Here, in particular Cederbaum, Scheipl, and Greven 2018 offers a method for efficient covariance smoothing using *tensor product P-splines* (see e.g. Fahrmeier et al. 2013, Chap. 8.2).

The aim of this thesis, as illustrated in Fig. 1.3, is to extend existing methods for elastic mean estimation of sparse and irregularly sampled curves, as proposed by Steyer, Stöcker, and Greven 2021 and implemented in the package `elasdics` (Steyer 2021) for the `R` programming language (R Core Team 2021), to also include invariance with respect to rotation and scaling. The later will be achieved by generalizing the concept of the full Procrustes mean from landmark to functional data and by iteratively applying full Procrustes mean estimation, rotation-alignment and parametrization-alignment, leading to the estimation of elastic full Procrustes means. Here, techniques

for Hermitian smoothing of the complex covariance surfaces as available in the `R` package `sparseFLMM` (Cederbaum, Volkmann, and Stöcker 2021) will be used.

The thesis is organized as follows. In Chapter 2 relevant background material is reviewed and the elastic full Procrustes mean is derived, in the case where curves $\beta : [0,1] \to \mathbb{R}^2$ are fully observed. In Chapter 3 an estimation procedure for the setting of sparse and irregularly observed curves $\beta(t_1), \ldots, \beta(t_m)$ is proposed, concluding the theoretical part of this thesis. In Chapter 4 the proposed methods will be verified and applied using simulated and empirical datasets. Finally, all results will be summarized in Chapter 5. Appendix A and Appendix B offer additional considerations and some reproducability guidelines.

2. Elastic Full Procrustes Means for Planar Curves

As a starting point, it is important to establish a notational and mathematical framework for the treatment of planar shapes. While the restriction to the 2D case might seem a major one, it still covers all shape data extracted from e.g. imagery and is therefore very applicable in practice. The outline of a 2D object may be naturally represented by a planar curve $\beta : [0,1] \to \mathbb{R}^2$ with $\beta(t) = (x_1(t), x_2(t))^\top$, where $x_1(t)$ and $x_2(t)$ are the scalar-valued *coordinate functions*. Calculations in two dimensions, and in particular the derivation of the full Procrustes mean, are greatly simplified by using complex notation. We will therefore identify $\mathbb{R}^2$ with $\mathbb{C}$, as shown in Fig. 2.1, and always use complex notation when representing a planar curve:

$$\beta : [0,1] \to \mathbb{C}, \quad \beta(t) = x_1(t) + \mathrm{i}x_2(t).$$

We will assume the curves to be absolutely continuous, denoted as $\beta \in \mathcal{AC}([0,1], \mathbb{C})$, guaranteeing that $\beta(t)$ has an integrable derivative. This is important when working in the square-root-velocity (SRV) framework, as will be discussed in Section 2.2. All considerations will be restricted to the case of open curves, with possible extensions to closed curves $\beta \in \mathcal{AC}(\mathbb{S}^1, \mathbb{C})$ discussed in **??**. Update

2.1. Equivalence Classes and Shape

As mentioned in the introduction, shape is usually defined by its invariance under the transformations of scaling, translation, and rotation. When considering the shape of curves, we additionally have to take into account invariance with respect to re-parametrisation. This can be seen, by noting that the curves $\beta(t)$ and $\beta(\gamma(t))$, with some re-parametrisation or *warping function* $\gamma : [0,1] \to [0,1]$ monotonically increasing and differentiable, have the same image and therefore represent the same geometrical object (see Fig. 1.1b). We can say that the actions of translation, scaling, rotation, and

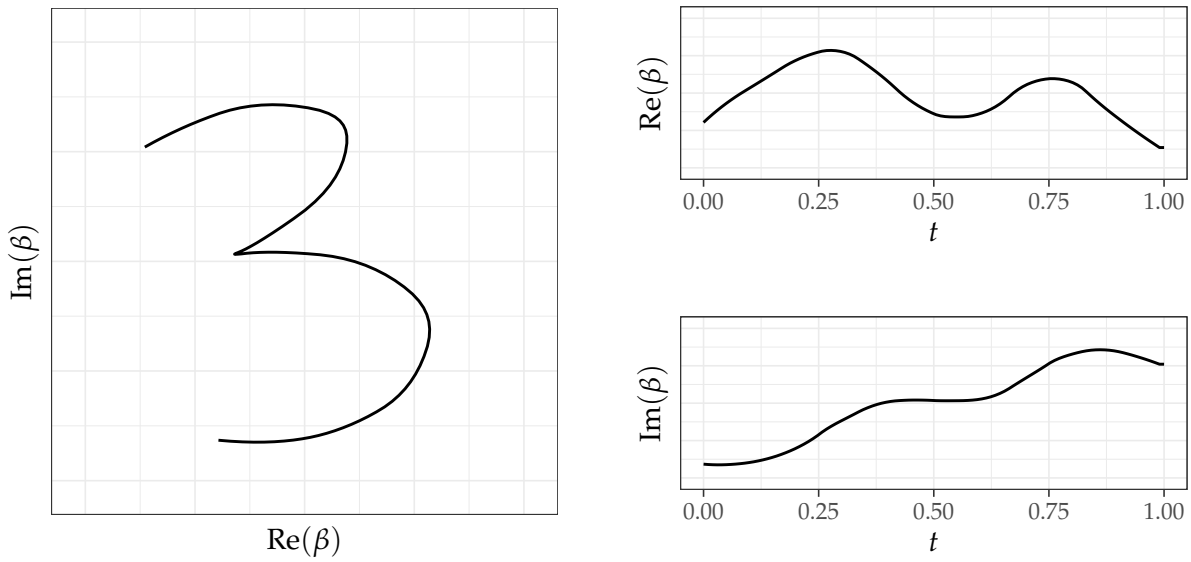

Figure 2.1.: Example of a planar curve (left) with respective coordinate functions (right) using complex notation, where $\mathrm{Re}(\beta) = x_1$ and $\mathrm{Im}(\beta) = x_2$ denote the *real* and *imaginary* parts of β. Data: see Fig. 1.1.

re-parametrisation are *equivalence relations* with respect to shape, as each action leaves the shape of the curve untouched and only changes the way it is represented. The shape of a curve can then be defined as the respective *equivalence class*, i.e. the set of all possible shape preserving transformations of the curve. As two equivalence classses are neccessarily either disjoint or identical, we can consider two curves as having the same shape, if they are elements of the same equivalence class (see Srivastava and Klassen 2016, p. 40).

When defining an equivalence class, one has to first consider how each individual transformation acts on a planar curve $\beta : [0,1] \to \mathbb{C}$. This is usually done using the notion of *group actions* and *product groups*, with the later desciribing multiple transformations acting at once. A brief introduction to group actions may be found in Srivastava and Klassen 2016, Chap. 3.

1. The *translation* group $\mathbb{C}$ acts on β by $(\xi, \beta) \overset{\mathrm{Trl}}{\longmapsto} \beta + \xi$, for any $\xi \in \mathbb{C}$. We can consider two curves as equivalent with respect to translation $\beta_1 \overset{\mathrm{Trl}}{\backsim} \beta_2$, if there exists a complex scalar $\widetilde{\xi} \in \mathbb{C}$ such that $\beta_1 = \beta_2 + \widetilde{\xi}$. Then, for some function β, the related equivalence class with respect to translation is given by $[\beta]_{\mathrm{Trl}} = \{\beta + \xi \,|\, \xi \in \mathbb{C}\}$.

2. The *scaling* group $\mathbb{R}^+$ acts on β by $(\lambda, \beta) \overset{\mathrm{Scl}}{\longmapsto} \lambda\beta$, for any $\lambda \in \mathbb{R}^+$. We define $\beta_1 \overset{\mathrm{Scl}}{\backsim} \beta_2$, if there exists a scalar $\widetilde{\lambda} \in \mathbb{R}^+$ such that $\beta_1 = \widetilde{\lambda}\beta_2$. An equivalence class

is $[\beta]_{\text{Scl}} = \{\lambda\beta \,|\, \lambda \in \mathbb{R}^+\}$.

3. The *rotation* group $[0, 2\pi)$ acts on β by $(\theta, \beta) \overset{\text{Rot}}{\longmapsto} e^{i\theta}\beta$, for any $\theta \in [0, 2\pi)$. We define $\beta_1 \overset{\text{Rot}}{\backsim} \beta_2$, if there exists a $\widetilde{\theta} \in [0, 2\pi)$ with $\beta_1 = e^{i\widetilde{\theta}}\beta_2$. An equivalence class is $[\beta]_{\text{Rot}} = \{e^{i\theta}\beta \,|\, \theta \in [0, 2\pi)\}$.

4. The *warping* group Γ acts on β by $(\gamma, \beta) \overset{\text{Wrp}}{\longmapsto} \beta \circ \gamma$, for any $\gamma \in \Gamma$ with Γ being the set of monotonically increasing and differentiable warping functions. We define $\beta_1 \overset{\text{Wrp}}{\backsim} \beta_2$, if there exists a warping function $\widetilde{\gamma} \in \Gamma$ with $\beta_1 = \beta_2 \circ \widetilde{\gamma}$. An equivalence class is $[\beta]_{\text{Wrp}} = \{\beta \circ \gamma \,|\, \gamma \in \Gamma\}$.

In a next step, we can consider how these transformations act in concert and whether they *commute*, i.e. whether the order of applying the transformations changes outcomes. Consider for example the actions of the *rotation and scaling* product group $\mathbb{R}^+ \times [0, 2\pi)$ given by $((\lambda, \theta), \beta) \overset{\text{Scl+Rot}}{\longmapsto} \lambda e^{i\theta}\beta$, which clearly commutes as $\lambda(e^{i\theta}\beta) = e^{i\theta}(\lambda\beta)$. On the other hand, the joint actions of *scaling and translation* do not commute, as $\lambda(\beta + \xi) \neq \lambda\beta + \xi$, with the same holding for the joint actions of *rotation and translation*. As the order of translating and rotating or scaling matters, one usually takes the translation to act on the already scaled and rotated curve. The joint action defined using this ordering is called an *Euclidean similarity transformation* with $((\xi, \lambda, \theta), \beta) \overset{\text{Eucl}}{\longmapsto} \lambda e^{i\theta}\beta + \xi$ (see Dryden and Mardia 2016, p. 62). Considering the action of *warping* or re-parametrization, we can note that it necessarily commutes with all Euclidean similarity transformations as those only act on the image of β, while the former only acts on the parametrization. Putting everything together we can give a formal definition of the shape of a planar curve as the following equivalence class:

Definition 2.1 (Shape)**.** The *shape* of an absolutely continous planar curve $\beta \in \mathcal{AC}([0, 1], \mathbb{C})$ is given by its equivalence class $[\beta]$ with respect to all Euclidean similarity transformations and re-parametrizations

$$[\beta] = \left\{\lambda e^{i\theta}(\beta \circ \gamma) + \xi \,|\, \xi \in \mathbb{C},\, \lambda \in \mathbb{R}^+,\, \theta \in [0, 2\pi),\, \gamma \in \Gamma\right\}.$$

The *shape space* $\mathcal{S}$ is then given by $\mathcal{S} = \{[\beta] \,|\, \beta \in \mathcal{AC}([0, 1],\, \mathbb{C})\}$.

2.2. The Elastic Full Procrustes Distance for Planar Curves

Let us now turn to the construction of an appropriate *shape distance* $d([\beta_1], [\beta_2])$ for two curves β_1, β_2. As the shapes $[\beta_1]$ and $[\beta_2]$ are elements of a non-Euclidean quotient space (the shape space $\mathcal{S}$), calculating a distance between them is not straight-forward. A common approach is to map each equivalence class $[\beta]$ to a suitable representative $\widetilde{\beta}$, so that the distance calculation in shape space can be identified with a (much simpler) distance calculation over the representatives in an underlying functional space.

To illustrate this, let us first discuss each type of shape-preserving transformation individually, starting with the Euclidean similarity transformations. Consider two equivalence classes with respect to translation $[\beta_1]_{\text{Trl}}, [\beta_2]_{\text{Trl}}$. They might be uniquely mapped to their centered elements $\widetilde{\beta}_i^{\text{Trl}} = \beta_i - \overline{\beta}_i \in [\beta_i]_{\text{Trl}}$ for $i = 1, 2$. The distance between the centered elements then defines a distance that is invariant under translation $d_{\text{Trl}}([\beta_1]_{\text{Trl}}, [\beta_2]_{\text{Trl}}) = \|\widetilde{\beta}_1^{\text{Trl}} - \widetilde{\beta}_2^{\text{Trl}}\|$, which is equal to the minimal distance when optimizing over the translation group. Similarly, a distance that is invariant under scaling might be defined over the normalized elements $\widetilde{\beta}_i^{\text{Scl}} = \frac{\beta_i}{\|\beta_i\|} \in [\beta_i]_{\text{Scl}}$ for $i = 1, 2$, as $d_{\text{Scl}}([\beta_1]_{\text{Scl}}, [\beta_2]_{\text{Scl}}) = \|\widetilde{\beta}_1^{\text{Scl}} - \widetilde{\beta}_i^{\text{Scl}}\|$. When considering invariance under rotation, we can first note that no "standardization" procedure compareable to normalizing and centering exists for the case of rotation. Instead of mapping $[\beta]_{\text{Rot}}$ to a fixed representative, we therefore have to identify an appropriate representative on a case-by-case basis. This can be achieved by defining the distance as the minimal distance $d_{\text{Rot}}([\beta_1]_{\text{Rot}}, [\beta_2]_{\text{Rot}}) = \min_{\widetilde{\beta}_2^{\text{Rot}} \in [\beta_2]_{\text{Rot}}} \|\beta_1 - \widetilde{\beta}_2^{\text{Rot}}\| = \min_{\theta \in [0, 2\pi)} \|\beta_1 - e^{i\theta}\beta_2\|$, when keeping one curve fixed and rotationally aligning the other curve (see e.g Stöcker and Greven 2021).

The Full Procrustes Distance

The three approaches can be combined to formulate the family of *Procrustes* distances, which are invariant under Euclidean similarity transform. The *partial Procrustes distance* is defined as the minimizing distance $d_{PP}([\beta_1]_{\text{Eucl}}, [\beta_2]_{\text{Eucl}}) = \min_{\theta \in [0, 2\pi)} \|\widetilde{\beta}_1 - e^{i\theta}\widetilde{\beta}_2\|$, when rotationally aligning the centered and normalized curves $\widetilde{\beta}_i = \frac{\beta_i - \overline{\beta}_i}{\|\beta_i - \overline{\beta}_i\|}$, $i = 1, 2$. On the other hand, the *full Procrustes distance* (see Definition 2.2) includes an additional alignment over scaling, leading to a slightly different geometrical interpretation (see

Dryden and Mardia 2016, pp. 77–78). Finally, the *Procrustes distance* given by $d_P([\beta_1]_{\text{Eucl}}, [\beta_2]_{\text{Eucl}}) = \arccos |\langle \widetilde{\beta}_1, \widetilde{\beta}_2 \rangle|$ defines a geodesic distance in the space of curves modulo Euclidean similarity transforms. As earlier approaches to elastic shape mean estimation, such as Srivastava, Klassen, et al. 2011, have been focused on calculating *intrinsic* means, they mostly use the Procrustes distance. Although no distance definition is inherently better than the other, in the context of mean estimation for sparse and irregular curves the full Procrustes distance might be slightly more suitable, as the additional scaling alignment offers more flexibility in a setting where—as will become clear later on—calculating a norm $\|\beta\| = \int_0^1 \|\beta(t)\| \, dt$ may already present a challenge. In this thesis, we will therefore only consider the full Procrustes distance and calculate *extrinsic* shape means. Note that in Definition 2.2 the optimization over scaling $\lambda \in \mathbb{R}^+$ and rotation $\theta \in [0, 2\pi)$ was combined into a single optimization over *rotation and scaling* $\omega = \lambda e^{i\theta} \in \mathbb{C}$.

Definition 2.2 (Full Procrustes distance)**.** The *full Procrustes distance* for two equivalence classes $[\beta_1]_{\text{Eucl}}$, $[\beta_2]_{\text{Eucl}}]$ is defined as

$$d_{FP}([\beta_1]_{\text{Eucl}}, [\beta_2]_{\text{Eucl}}) = \min_{\omega \in \mathbb{C}} \|\widetilde{\beta}_1 - \omega \widetilde{\beta}_2\| \tag{2.1}$$

with centered and normalized representatives $\widetilde{\beta}_i = \frac{\beta_i - \overline{\beta}_i}{\|\beta_i - \overline{\beta}_i\|}$.

By using a similar proof for complex-valued landmark data in Dryden and Mardia 2016, Chap 8 as a blueprint, we can show that Eq. (2.1) has the following analytical solution.

Lemma 2.1. *Let $\beta_1, \beta_2 : [0,1] \to \mathbb{C}$ be two planar curves with corresponding equivalence classes $[\beta_1]_{Eucl}, [\beta_2]_{Eucl}$ with respect to Euclidean similarity transforms and let $\widetilde{\beta}_i = \frac{\beta_i - \overline{\beta}_i}{\|\beta_i - \overline{\beta}_i\|}$.*

i.) *The full Procrustes distance between $[\beta_1]_{Eucl}$ and $[\beta_2]_{Eucl}$ is given by*

$$d_{FP}([\beta_1]_{Eucl}, [\beta_2]_{Eucl}) = \sqrt{1 - \langle \widetilde{\beta}_1, \widetilde{\beta}_2 \rangle \langle \widetilde{\beta}_2, \widetilde{\beta}_1 \rangle} \tag{2.2}$$

ii.) *The optimal rotation and scaling alignment of $\widetilde{\beta}_2$ onto $\widetilde{\beta}_1$ is given by $\omega^{opt} = \langle \widetilde{\beta}_2, \widetilde{\beta}_1 \rangle$. The aligned curve $\widetilde{\beta}_2^P = \langle \widetilde{\beta}_2, \widetilde{\beta}_1 \rangle \cdot \widetilde{\beta}_2$ is then called the* Procrustes fit *of $\widetilde{\beta}_2$ onto $\widetilde{\beta}_1$.*

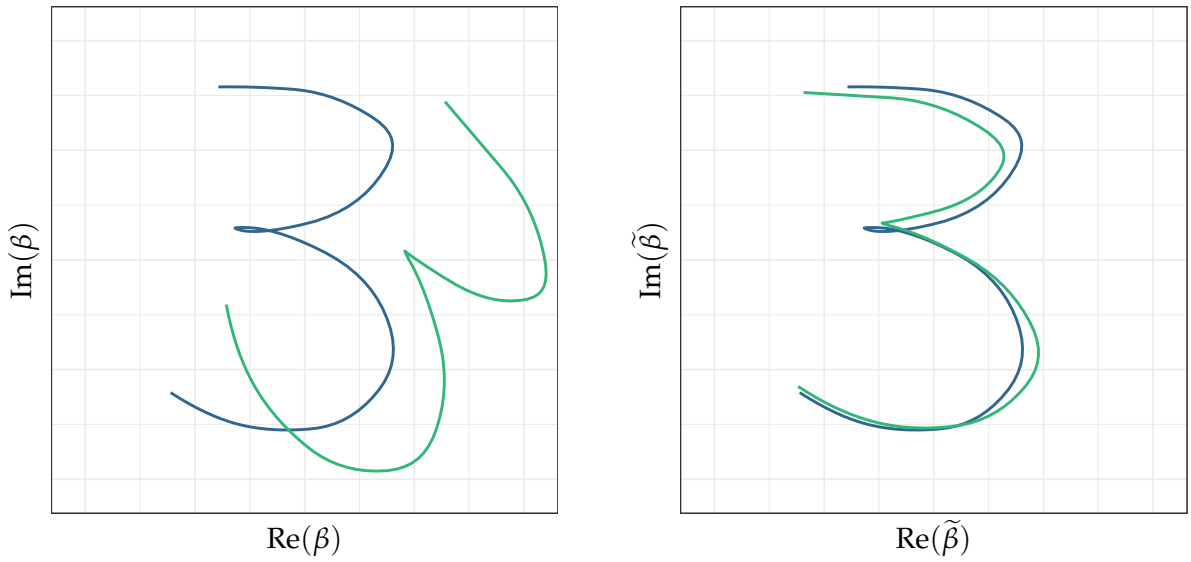

Figure 2.2.: Procrustes fit (right; normalized and centered) of two example curves (left). The Procrustes fit of β_2 (green) onto β_1 (blue) is given by $\widetilde{\beta}_2^p = \langle \widetilde{\beta}_2, \widetilde{\beta}_1 \rangle \widetilde{\beta}_2$. Data: See Fig. 1.1.

Proof. See Appendix A.1.1. □

Fig. 2.2 shows an example of two curves that where aligned by minimizing their full Procrustes distance using Lemma 2.1.

The Elastic Distance

When considering warping, we would like to do something similar to rotation in trying to find an optimal warping alignment between two curves β_1, β_2 by optimizing their distance over the space of warping functions Γ. A usual choice would be to optimize over the $\mathbb{L}^2$-distance by $\inf_{\gamma \in \Gamma} \|\beta_1 - \beta_2 \circ \gamma\|_{\mathbb{L}^2}$, where the $\mathbb{L}^2$-norm and scalar-product are given by $\|f\|_{\mathbb{L}^2} = \sqrt{\int_0^1 \overline{f(t)} f(t) \, \mathrm{d}t}$ and $\langle f, g \rangle_{\mathbb{L}^2} = \int_0^1 \overline{f(t)} g(t) \, \mathrm{d}t$ with $\bar{z} = \mathrm{Re}(z) - \mathrm{i}\mathrm{Im}(z)$ denoting the complex conjugate of $z \in \mathbb{C}$. However, as optimizing over re-parametrization using the $\mathbb{L}^2$-distance has problems relating to the so called *pinching effect* and *inverse-inconsistency*, this does not define a proper distance. Here, the later means that aligning the parametrization of one curve to another by $\inf_{\gamma \in \Gamma} \|\beta_1 - \beta_2 \circ \gamma\|_{\mathbb{L}^2}$ may yield different results than $\inf_{\gamma \in \Gamma} \|\beta_2 - \beta_1 \circ \gamma\|_{\mathbb{L}^2}$ (see Srivastava and Klassen 2016, pp. 88–90).

A solution proposed in Srivastava, Klassen, et al. 2011 is to replace the $\mathbb{L}^2$-distance with an *elastic distance*, on which warping acts by isometry. Calculation of

this metric, the Fisher-Rao Riemannian metric (Rao 1945), can be greatly simplified by using the *square-root-velocity* (SRV) framework, as the Fisher-Rao metric of two curves can be equivalently calculated as the $\mathbb{L}^2$-distance of their respective SRV curves. As this SRV representation makes use of derivatives, any curve β that has a SRV curve must fulfill some kind of differentiability constraint. Here it is enough to consider only curves that are absolutely continuous $\beta \in \mathcal{AC}([0,1], \mathbb{C})$, which in particular means that the original curves do not have to be smooth but might also be, e.g.,piecewise linear (see Srivastava and Klassen 2016, p. 91). Note that, because of the use of derivatives, any elastic analysis of curves will automatically be translation invariant as well. See Fig. 2.3 for an example SRV curve of a digit '3'.

Definition 2.3 (Elastic distance (Srivastava, Klassen, et al. 2011))**.** The *elastic distance* between equivalence classes $[\beta_1]_{\text{Wrp+Trl}}$, $[\beta_2]_{\text{Wrp+Trl}}$ is defined as

$$d_E([\beta_1]_{\text{Wrp+Trl}}, [\beta_2]_{\text{Wrp+Trl}}) = \inf_{\gamma \in \Gamma} \|q_1 - (q_2 \circ \gamma) \cdot \sqrt{\dot{\gamma}}\|_{\mathbb{L}^2} \tag{2.3}$$

with the respective *square-root-velocity* (SRV) representations $q_i \in \mathbb{L}^2([0,1], \mathbb{C})$ given by

$$q_i(t) = \begin{cases} \frac{\dot{\beta}_i(t)}{\sqrt{\|\dot{\beta}_i(t)\|}} & \text{for} \quad \dot{\beta}_i(t) \neq 0, \\ 0 & \text{for} \quad \dot{\beta}_i(t) = 0, \end{cases} \tag{2.4}$$

where $\beta_i \in \mathcal{AC}([0,1], \mathbb{C})$ and $\dot{\beta}_i(t) = \frac{\mathrm{d}\beta_i(t)}{\mathrm{d}t}$ for $i = 1, 2$.

Unlike the optimization over rotation in the definition of the full Procrustes distance, no analytical solution exists for the optimization over warping in Eq. (2.3). Instead, it is usually solved numerically, by minimizing a cost function $H[\gamma] = \int_0^1 \|q_1(t) - q_2(\gamma(t)) \sqrt{\dot{\gamma}(t)}\| \, \mathrm{d}t$ using a dynamic programming algorithm (see e.g. Srivastava and Klassen 2016, p. 152) or gradient based methods (see e.g. Steyer, Stöcker, and Greven 2021).

The Elastic Full Procrustes Distance

When the original curves β are absolutely continuous, the SRV curves are always ensured to be $\mathbb{L}^2$-integrable. As a consequence, we can re-construct the original

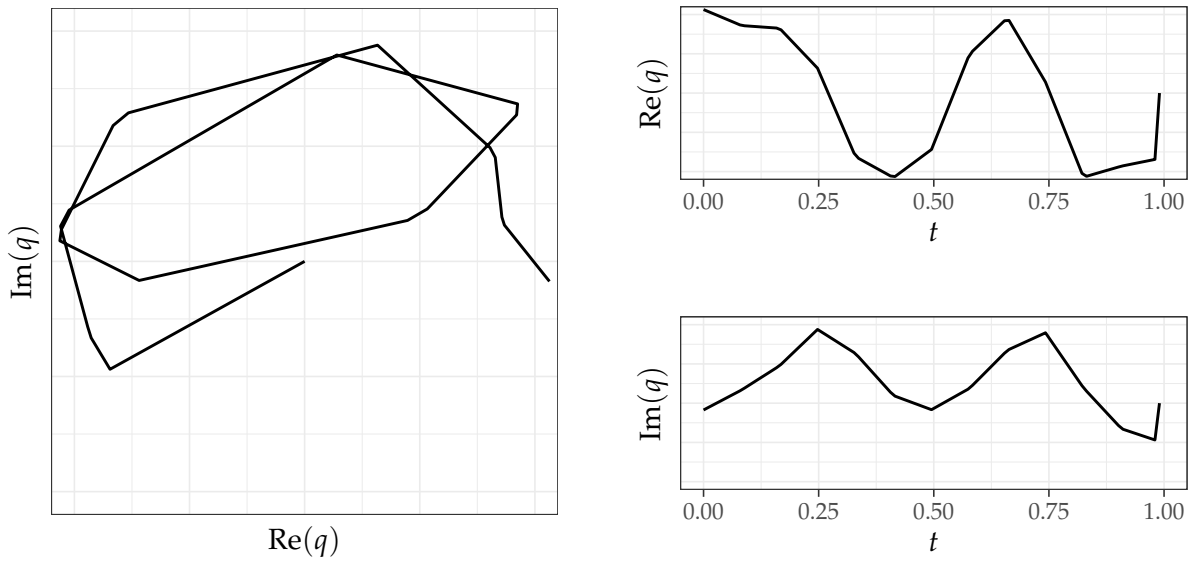

Figure 2.3.: SRV function (left) of the planar curve in Fig. 2.1 with respective SRV coordinate functions (right). Note that the polygon-like look of the SRV curve is an artifact of the (linear) smoothing applied to the original data on SRV level (see Appendix A.2). Data: see Fig. 1.1.

curve β up to translation from its respective SRV curve q by integration $\beta(t) = \beta(0) + \int_0^t q(s)\|q(s)\|ds$. Because the translation of the original curve is usually not of interest from the point of shape analysis, the SRV curve holds all relevant information about the shape of β. This means, in particular, that instead of analysing the shape of β, we can equivalently analyse the shape of q. The shape preserving transformations on original curve level translate to SRV curve level by actions laid out in Lemma 2.2.

Lemma 2.2. *The actions of the translation, scaling, rotation, and re-parametrization groups commute on SRV level. Furthermore, the individual transformations translate to SRV level by*

$$\textit{i.)}\ (\xi, q) \overset{Trl}{\longmapsto} q, \quad \textit{ii.)}\ (\lambda, q) \overset{Scl}{\longmapsto} \sqrt{\lambda} q, \quad \textit{iii.)}\ (\theta, q) \overset{Rot}{\longmapsto} e^{i\theta} q, \quad \textit{iv.)}\ (\gamma, q) \overset{Wrp}{\longmapsto} (q \circ \gamma)\sqrt{\dot{\gamma}}$$

(see e.g. Srivastava *and* Klassen *2016, p. 142).*

Proof. The SRVF $\widetilde{q}(t)$ of $\widetilde{\beta}(t) = \lambda e^{i\theta} \beta(\gamma(t)) + \xi$ is given by

$$\widetilde{q}(t) = \frac{\lambda e^{i\theta} \dot{\beta}(\gamma(t))\, \dot{\gamma}(t)}{\sqrt{||\lambda e^{i\theta} \dot{\beta}(\gamma(t))\, \dot{\gamma}(t)||}} = \sqrt{\lambda} e^{i\theta} \frac{\dot{\beta}(\gamma(t))}{\sqrt{||\dot{\beta}(\gamma(t))\,||}} \sqrt{\dot{\gamma}(t)} = \sqrt{\lambda} e^{i\theta} (q \circ \gamma) \sqrt{\dot{\gamma}(t)}.$$

The result is irrespective of the order of applying the transformations. □

We can note that the SRV curves are invariant under translation of the original curves, that the rotation is preserved on the SRV level, that scaling translates to SRV level by $\sqrt{\cdot}$. It is in particular noteworthy, that warping the original curve changes the image of the SRV curve.

Going forward, we will work in the SRV framework and combine the elastic distance with the full Procrustes distance. While the full Procrustes distance (see Definition 2.2) was defined over the normalized and centered curves, the SRV curves are already translation invariant so additional centering is not necessary (see Lemma 2.2 i.). We will therefore define the *elastic full Procrustes distance* as the minimal distance, when aligning the scaling, rotation, and warping of the normalized SRV curves $\widetilde{q} = \frac{q}{\|q\|}$. Note that when the original curve β is of unit length $L[\beta] = \int_0^1 |\dot{\beta}(t)| \, \mathrm{d}t = 1$ the SRV curve $q = \frac{\dot{\beta}}{\sqrt{|\dot{\beta}|}}$ will be normalized, as

$$\|q\| = \sqrt{\int_0^1 |q(t)|^2 \, \mathrm{d}t} = \sqrt{\int_0^1 |\dot{\beta}(t)| \, \mathrm{d}t} = \sqrt{L[\beta]}. \tag{2.5}$$

Definition 2.4 (Elastic full Procrustes distance)**.** The *elastic full Procrustes distance* between shapes $[\beta_1]$, $[\beta_2]$ of two continuously differentiable planar curves β_1, $\beta_2 \in \mathcal{AC}([0,1], \mathbb{C})$ is given by

$$d([\beta_1], [\beta_2]) = \inf_{\omega \in \mathbb{C}, \, \gamma \in \Gamma} \|\widetilde{q}_1 - \omega(\widetilde{q}_2 \circ \gamma)\sqrt{\dot{\gamma}}\|_{\mathbb{L}^2}, \tag{2.6}$$

with normalized SRV representation $\widetilde{q}_i = \frac{q_i}{\|q_i\|} \in \mathbb{L}^2([0,1], \mathbb{C})$, where q_i is the SRV representation of β_i, for $i = 1, 2$.

To calculate the elastic full Procrustes distance, we need to solve the joint optimization problem over $\mathbb{C} \times \Gamma$

$$(\omega^{\mathrm{opt}}, \gamma^{\mathrm{opt}}) = \operatorname*{argmin}_{\omega \in \mathbb{C}, \, \gamma \in \Gamma} \|\widetilde{q}_1 - \omega(\widetilde{q}_2 \circ \gamma)\sqrt{\dot{\gamma}}\|_{\mathbb{L}^2}, \tag{2.7}$$

so that the elastic full Procrustes distance is given as the $\mathbb{L}^2$-distance of the optimally aligned normalized SRV curves

$$d([\beta_1], [\beta_2]) = \|\widetilde{q}_1 - \omega^{\mathrm{opt}}(\widetilde{q}_2 \circ \gamma^{\mathrm{opt}})\sqrt{\dot{\gamma}^{\mathrm{opt}}}\|_{\mathbb{L}^2}. \tag{2.8}$$

Following Srivastava, Klassen, et al. 2011 we adapt an iterative procedure, where in each step k we optimize over the sets of parameters individually, iterating through both solutions until some form of convergence is reached. Let us first consider the optimization over $\omega \in \mathbb{C}$ for a fixed $\gamma^{(k)} \in \Gamma$.

Γ nicht vollständig.

$$\omega^{(k)} = \underset{\omega \in \mathbb{C}}{\operatorname{argmin}} \, \| \widetilde{q}_1 - \omega (\widetilde{q}_2 \circ \gamma^{(k)}) \sqrt{\dot{\gamma}^{(k)}} \|_{\mathbb{L}^2} \,, \tag{2.9}$$

Eq. (2.9) is equivalent to the optimization problem of the full Procrustes distance defined in Definition 2.2. Following Lemma 2.1 ii.), the solution is given by the Procrustes fit of $(\widetilde{q}_2 \circ \gamma^{(k)}) \sqrt{\dot{\gamma}^{(k)}}$ onto $\widetilde{q}_1$ with

$$\omega^{(k)} = \langle (\widetilde{q}_2 \circ \gamma^{(k)}) \sqrt{\dot{\gamma}^{(k)}}, \widetilde{q}_1 \rangle \tag{2.10}$$

For fixed rotation and scaling $\omega^{(k)} \in \mathbb{C}$ the optimization problem over $\gamma \in \Gamma$ is given by

$$\gamma^{(k+1)} = \underset{\gamma \in \Gamma}{\operatorname{arginf}} \, \| \widetilde{q}_1 - (\omega^{(k)} \widetilde{q}_2 \circ \gamma) \sqrt{\dot{\gamma}} \|_{\mathbb{L}^2} \,. \tag{2.11}$$

Again,Eq. (2.11) is equivalent to the optimization problem of the elastic distance defined in Definition 2.3, when aligning the parametrization of the normalized SRV curve $\widetilde{q}_1$ and the rotation and scaling aligned, normalized SRV curve $\omega^{(k)} q_2$. A solution $\gamma^{(k+1)}$ can be found by applying known optimization techniques such as a dynamical programming algorithm or a gradient based method. In this thesis we will use the methods laid out in Steyer, Stöcker, and Greven 2021 and implemented in the `R` package `elasdics` (Steyer 2021) for solving Eq. (2.11) in the setting of sparse and irregularly sampled curves.

Algorithm 2.1 (Elastic full Procrustes distance). *β_1, β_2 absolutely continous planar curves with SRV curves $q_1, q_2 \in \mathbb{L}^2([0,1], \mathcal{C})$ and normalized SRV curves $\widetilde{q}_i = \frac{q_i}{\|q_i\|}$. Set $\gamma^{(0)}(t) = t$ as the initial parametrization alignment. Set $k = 0$.*

1. *Set $\widetilde{q}^{(k)} = (\widetilde{q} \circ \gamma^{(k)}) \sqrt{\dot{\gamma}^{(k)}}$*
2. *Calculate $\omega^{(k)} = \langle \widetilde{q}_2^{(k)}, \widetilde{q}_1 \rangle$. **Stop** if $k > 1$ and $\| \omega^{(k)} \widetilde{q}^{(k)} - \omega^{(k-1)} \widetilde{q}^{(k-1)} \| < \epsilon$*
3. *Solve $\gamma^{(k+1)} = \operatorname{argmin}_{\gamma \in \Gamma} \| \widetilde{q}_1 - (\omega^{(k)} \cdot \widetilde{q}_2 \circ \gamma) \sqrt{\dot{\gamma}} \|_{\mathbb{L}^2}$.*
4. *Set $k = k + 1$ and return to Step 1.*

The elastic full Procrustes distance is given as $d([\beta_1],[\beta_2]) = \|\widetilde{q}_1 - \omega^{(k)}(\widetilde{q}_2 \circ \gamma^{(k)})\sqrt{\dot{\gamma}^{(k)}}\|_{\mathbb{L}^2}$.

2.3. The Elastic Full Procrustes Mean for Planar Curves

We now want to use the elastic Full Procrustes distance to calculate shape means for sets of planar curves. Again, we assume all curves to be absolutely continous $\beta_i \in \mathcal{AC}([0,1], \mathbb{C})$ with corresponding SRV curves $q_i \in \mathbb{L}^2([0,1], \mathbb{C})$, $i = 1, \ldots, N$. We can take into account invariance with respect to shape-preserving transformations by defining the mean as a minimizer over the sum of squared elastic full Procrustes distances between the shape of each curve and a mean shape. If the resulting mean is a global minimum, it is usually called a "sample Fréchet mean" (Fréchet 1948), if it is a local minimum a "sample Karcher mean" (Karcher 1977) (see Dryden and Mardia 2016, p. 111).

Definition 2.5 (Elastic full Procrustes mean)**.** For a set of curves $\beta_i \in \mathcal{AC}([0,1], \mathbb{C})$, $i = 1, \ldots, N$, their *elastic full Procrustes mean* is given by a minimizing shape $[\hat{\mu}]$ with

$$[\hat{\mu}] = \operatorname*{arginf}_{[\mu]\in\mathcal{S}} \sum_{i=1}^{N} d_{EF}([\mu],[\beta_i])^2\,, \tag{2.12}$$

where $\mathcal{S} = \{[\beta] : \beta \in \mathcal{AC}([0,1], \mathbb{C})\}$ is the shape space.

In practice, we will always solve Eq. (2.12) directly on SRV level, by using the definition of the elastic full Procrustes distance (see Definition 2.4) and writing it as an optimization problem over a normalized SRV mean function.

$$\hat{\mu}_q = \operatorname*{argmin}_{\mu_q\in\mathbb{L}^2,\, \|\mu_q\|=1} \sum_{i=1}^{N} \left(\inf_{\omega_i\in\mathbb{C},\gamma_i\in\Gamma} \|\mu_q - \omega_i(\widetilde{q}_i \circ \gamma_i)\sqrt{\dot{\gamma}_i}\| \right)^2 . \tag{2.13}$$

The estimated normalized SRV mean $\hat{\mu}_q$ then defines a representative unit-length mean $\hat{\mu} \in [\hat{\mu}]$ by integration $\hat{\mu}(t) = \hat{\mu}(0) + \int_0^t \hat{\mu}_q(s)\|\hat{\mu}_q(s)\|\,ds$ (compare Eq. (2.5)), which is unique up to translation $\hat{\mu}(0)$. When re-constructing $\hat{\mu}$ from $\hat{\mu}_q$, one may decide to set $\hat{\mu}(0)$ to a certain value depending on the application. In particular, setting $\hat{\mu}(0) = 0$, so that the mean curve starts at the origin, makes sense when the object represented by the mean curve has a 'natural' starting point shared across all objects of this type. An

example, explored in Section 4.4 are tounge shapes, which all connect to the back of the mouth on one end. Another possibility would be to choose a $\hat{\mu}(0)$ that centers the mean curve, by setting $\hat{\mu}(0) = \int_0^1 \int_0^t \hat{\mu}_q(s)\|\hat{\mu}_q(s)\| \, ds \, dt$. From the point of shape analysis, the choice of representation does not make a difference, as both mean curves are elements of $[\hat{\mu}]$ and therefore have the same shape. However, the distinction becomes important when the estimated mean curve $\hat{\mu}$ is used in concert with other curves, for example in visualizing multiple curves or in comparing multiple class mean shapes, as those do not typically share the same center or starting point.

Turning back to the calculation of $\hat{\mu}_1$, we can simplify Eq. (2.13) by applying the following Lemma, which uses the analytical solution for the optimization over rotation in the full Procrustes distance (see Lemma 2.1 i.).

Lemma 2.3. *Let β_1, β_2 be two absolutely continuous planar curves with corresponding shape $[\beta_1], [\beta_2]$. Let $\widetilde{q}_1, \widetilde{q}_2$ be the respective normalized SRV curves. The elastic full Procrustes distance is given by*

$$d([\beta_1], [\beta_2]) = \inf_{\gamma \in \Gamma} \quad \sqrt{1 - \langle \widetilde{q}_1, (\widetilde{q}_2 \circ \gamma)\sqrt{\dot{\gamma}} \rangle \langle (\widetilde{q}_2 \circ \gamma)\sqrt{\dot{\gamma}}, \widetilde{q}_1 \rangle} \tag{2.14}$$

Proof. This follows from applying Lemma 2.1 i.) to Eq. (2.6), keeping γ fixed. □

Then Eq. (2.13) can be rewritten as

$$\hat{\mu}_q = \operatorname*{argmin}_{\mu_q \in \mathbb{L}^2, \|\mu_q\|=1} \sum_{i=1}^{N} \inf_{\gamma_i \in \Gamma} \left(1 - \langle \mu_q, \, (\widetilde{q}_i \circ \gamma_i)\sqrt{\dot{\gamma}_i} \rangle \langle (\widetilde{q}_i \circ \gamma_i)\sqrt{\dot{\gamma}_i}, \, \mu_q \rangle\right) \tag{2.15}$$

$$\hat{\mu}_q = \operatorname*{argmax}_{\mu_q \in \mathbb{L}^2, \|\mu_q\|=1} \sum_{i=1}^{N} \sup_{\gamma_i \in \Gamma} \langle \mu_q, \, (\widetilde{q}_i \circ \gamma_i)\sqrt{\dot{\gamma}_i} \rangle \langle (\widetilde{q}_i \circ \gamma_i)\sqrt{\dot{\gamma}_i}, \, \mu_q \rangle \tag{2.16}$$

and we end up with a two step optimization problem consisting of an outer optimization over μ_q and an inner optimization over the set $\{\gamma_i\}_{i=1,\ldots,N}$. Similarly to the approaches discussed in Srivastava and Klassen 2016 and to Steyer, Stöcker, and Greven 2021, we solve this iteratively by iterative *template based alignment* (see e.g. Srivastava and Klassen 2016, p. 271): In each step, the mean $\hat{\mu}_q$ is estimated while keeping the parametrizations γ_i fixed, after which the γ_i are updated by calculating the warping alignment of the full Procrustes fit of each $\widetilde{q}_i$ onto $\hat{\mu}_q$.[1] Mean estimation

[1] Note that this is *not* the same as performing an elastic full Procrustes fit of $\widetilde{q}_i$ onto $\hat{\mu}_q$ in each step k,

and warping alignment are iterated until the mean shape has converged.

Let us consider the outer optimization problem in step k for a fixed set of warping functions $\{\gamma_i^{(k)}\}_{i=1,\dots,N}$ with corresponding warping aligned normalized SRV curves $\widetilde{q}_i^{(k)} = (\widetilde{q}_i \circ \gamma_i^{(k)})\sqrt{\dot{\gamma}_i^{(k)}}$. Note that if no warping alignment has happened yet, we can always set $\gamma_i^{(0)}(t) = t$ for all $i = 1, \dots, N$ as a starting value. The problem we have to solve is

$$\hat{\mu}_q^{(k)} = \underset{\mu_q \in \mathbb{L}^2,\, \|\mu_q\|=1}{\operatorname{argmax}} \sum_{i=1}^{N} \left\langle \mu_q, \widetilde{q}_i^{(k)} \right\rangle \left\langle \widetilde{q}_i^{(k)}, \mu_q \right\rangle . \tag{2.17}$$

We can reformulate this by writing out the complex functional scalar products $\langle f, g \rangle = \int_0^1 \overline{f(t)} g(t)\, \mathrm{d}t$ for functions $f, g \in \mathbb{L}^2([0,1], \mathbb{C})$, where $\overline{f(t)}$ denotes the complex conjugate of $f(t)$.

$$\hat{\mu}_q^{(k)} = \underset{\mu_q \in \mathbb{L}^2,\, \|\mu_q\|=1}{\operatorname{argmax}} \sum_{i=1}^{N} \int_0^1 \int_0^1 \overline{\mu_q(s)} \widetilde{q}_i^{(k)}(s) \overline{\widetilde{q}_i^{(k)}(t)} \mu_q(t)\, \mathrm{d}s\, \mathrm{d}t \tag{2.18}$$

$$\hat{\mu}_q^{(k)} = \underset{\mu_q \in \mathbb{L}^2,\, \|\mu_q\|=1}{\operatorname{argmax}} \int_0^1 \int_0^1 \overline{\mu_q(s)} \left(\sum_{i=1}^{N} \widetilde{q}_i^{(k)}(s) \overline{\widetilde{q}_i^{(k)}(t)} \right) \mu_q(t)\, \mathrm{d}s\, \mathrm{d}t \tag{2.19}$$

We can identify the inner term as proportional to a sample estimator $\check{C}^{(k)}(s,t) = \frac{1}{N} \sum_{i=1}^{N} \widetilde{q}_i^{(k)}(s) \overline{\widetilde{q}_i^{(k)}(t)}$ of the population covariance surface of the normalized SRV curves $C^{(k)}(s,t) = \mathbb{E}[\widetilde{q}^{(k)}(s) \overline{\widetilde{q}^{(k)}(t)}]$, when noting that $\mathbb{E}[\widetilde{q}^{(k)}(t)] = 0$ for all $t \in [0,1]$ due to rotational symmetry.

$$\hat{\mu}_q^{(k)} = \underset{\mu_q \in \mathbb{L}^2,\, \|\mu_q\|=1}{\operatorname{argmax}} N \cdot \int_0^1 \int_0^1 \overline{\mu_q(s)} \check{C}^{(k)}(s,t) \mu_q(t)\, \mathrm{d}s\, \mathrm{d}t \tag{2.20}$$

By replacing $\check{C}^{(k)}(s,t)$ by its expectation $C^{(k)}(s,t)$, we can analogously formulate an estimator on the population level.

$$\mathbb{E}[\mu_q^{(k)}] = \underset{\mu_q \in \mathbb{L}^2 \colon \|\mu_q\|=1}{\operatorname{argmax}} \int_0^1 \int_0^1 \overline{\mu_q(s)} C^{(k)}(s,t) \mu_q(t)\, \mathrm{d}s\, \mathrm{d}t \tag{2.21}$$

We can rewrite this again as a functional scalar product by considering the *covariance operator* C with $(C\mu_q)(s) = \int_0^1 C(s,t)\mu_q(t)\, \mathrm{d}t$ (see Ramsay and Silverman 2005,

because the warping and Procrustes alignments are themselves not iterated over.

p. 153).

$$\mathbb{E}[\mu_q^{(k)}] = \underset{\mu_q \in \mathbb{L}^2, \|\mu_q\|=1}{\operatorname{argmax}} \left\langle \mu_q, C^{(k)} \mu_q \right\rangle \tag{2.22}$$

This is a well known problem in the context of functional principal component analysis (FPCA), but typically only for real-valued covariance operators. From $\overline{C(s,t)} = \overline{\mathbb{E}[\widetilde{q}(s)\overline{\widetilde{q}(t)}]} = \mathbb{E}[\widetilde{q}(t)\overline{\widetilde{q}(s)}] = C(t,s)$ it follows that $\langle \mu_q, C\mu_q \rangle = \langle C\mu_q, \mu_q \rangle$ and therefore that C is a *self-adjoint* operator. The optimization problem then reduces to an eigenfunction problem

$$C^{(k)} u^{(k)} = \lambda^{(k)} u^{(k)} \quad \Leftrightarrow \quad \int_0^1 C^{(k)}(s,t) u^{(k)}(t)\, dt = \lambda^{(k)} u^{(k)}(s)\,, \tag{2.23}$$

where $\lambda^{(k)} = \left\langle \mu_q, C^{(k)} \mu_q \right\rangle$ is the target function to maximize. For normalized eigenfunctions $u_1^{(k)}, u_2^{(k)}, \ldots$ and corresponding eigenvalues $\lambda_1^{(k)} \geq \lambda_2^{(k)} \geq \ldots$ of $C^{(k)}(s,t)$, the expectation $\mathbb{E}[\hat{\mu}_q^{(k)}(t)]$ is given by the leading normalized eigenfunction $u_1^{(k)}(t)$ of $C^{(k)}(s,t)$ (see Ramsay and Silverman 2005, pp. 153, 397).

We will estimate $C^{(k)}(s,t)$ using the methods for covariance estimation from sparse and irregular observations laid out in Chapter 3. Given such an estimate $\hat{C}^{(k)}(s,t)$, we can calculate the elastic full Procrustes mean by the following algorithm.

Algorithm 2.2 (Elastic full Procrustes mean)**.** *Let $\{\beta_i\}_{i=1,\ldots,N}$ be a set of planar curves with corresponding SRV curves $\{q_i\}_{i=1,\ldots,N}$. Let $\widetilde{q}_i = \frac{q_i}{\|q_i\|}$. Set $\gamma_i^0(t) = t$ for all $i = 1, \ldots, N$ as the initial parametrisation alignment. Set $k = 0$.*

1. *For $i = 1, \ldots, N$: Set $\widetilde{q}_i^{(k)} = \left(\widetilde{q}_i \circ \gamma_i^{(k)}\right) \cdot \sqrt{\dot{\gamma}_i^{(k)}}$.*
2. *Estimate $\hat{C}^{(k)}(s,t)$ from $\left\{\widetilde{q}_i^{(k)}\right\}_{i=1,\ldots,N}$.*
3. *Estimate $\hat{u}_1^{(k)}$ by eigendecomposition of $\hat{C}^{(k)}(s,t)$.*
4. *Set $\hat{\mu}_q^{(k)}$ as $\hat{u}_1^{(k)}$.* **Stop** *if $k > 1$ and $\|\hat{\mu}_q^{(k)} - \hat{\mu}_q^{(k-1)}\| < \epsilon$.*
5. *For $i = 1, \ldots, N$: Calculate $\omega_i^{(k)} = \left\langle \widetilde{q}_i^{(k)}, \hat{\mu}_q^{(k)} \right\rangle$.*
6. *For $i = 1, \ldots, N$: Solve $\gamma_i^{(k+1)} = \operatorname{argmin}_{\gamma \in \Gamma} \|\hat{\mu}_q^{(k)} - \omega_i^{(k)} (\widetilde{q}_i \circ \gamma) \sqrt{\dot{\gamma}}\|$.*
7. *Set $k = k + 1$ and return to Step 1.*

3. Mean Estimation for Sparse and Irregular Observations

So far, we have considered estimation of the elastic full Procrustes mean in a setting, where each curve β_i is assumed fully observed. This is usually not the case in practice, as each observation β_i may itself only be observed at a finite number of discrete points $\beta_i(t_{i1}), \ldots, \beta_i(t_{in_i})$. Additionally, the number of observed points per curve n_i might be quite small and the points do not need to follow a common sampling scheme across all curves, a setting which is respectively known as *sparse* and *irregular*.

Following the steps laid out in Algorithm 2.2, this chapter proposes a mean estimation strategy for dealing with sparse and irregular observations. In a first step, the construction of SRV and warped SRV curves from discrete (and possibly sparse) observations will be shown in Section 3.1. Section 3.2 discusses efficient estimation of the complex covariance surface $C^{(k)}(s,t)$ from sparse observations. In Section 3.3, calculation of the leading eigenfunction $\hat{u}_1^{(k)}$ of $C^{(k)}(s,t)$ in a fixed basis will be shown. Section 3.4 deals with the estimation of the optimal rotation and scaling alignment $\omega_i^{(k)} = \langle \widetilde{q}_i^{(k)}, \hat{\mu}_q^{(k)} \rangle$, where $\widetilde{q}_i^{(k)}$ is a sparsely observed normalized SRV curve, while $\hat{\mu}_q^{(k)}$ is a smooth SRV mean function. Note that the final warping alignment step in Algorithm 2.2 is solved by using methods for warping alignment of sparse and irregular curves provided in Steyer, Stöcker, and Greven 2021.

3.1. Discrete Treatment of SRV Curves

As a first step, we need to calculate the *normalized SRV curves* $\widetilde{q}_i = \frac{q}{\|q\|}$ from sparse observations. As the SRV curve of $\beta \in \mathcal{AC}([0,1], \mathbb{C})$ is defined as $q = \dot{\beta} / \sqrt{\|\dot{\beta}\|}$ (for $\dot{\beta} \neq 0$), we have to be able to calculate a derivate of β. However, as we never observe the whole function β but only a discrete set of points $\beta(t_1), \ldots, \beta(t_n)$, as seen in Fig. 3.1, we cannot simply calculate a pointwise derivative. Following Steyer, Stöcker, and

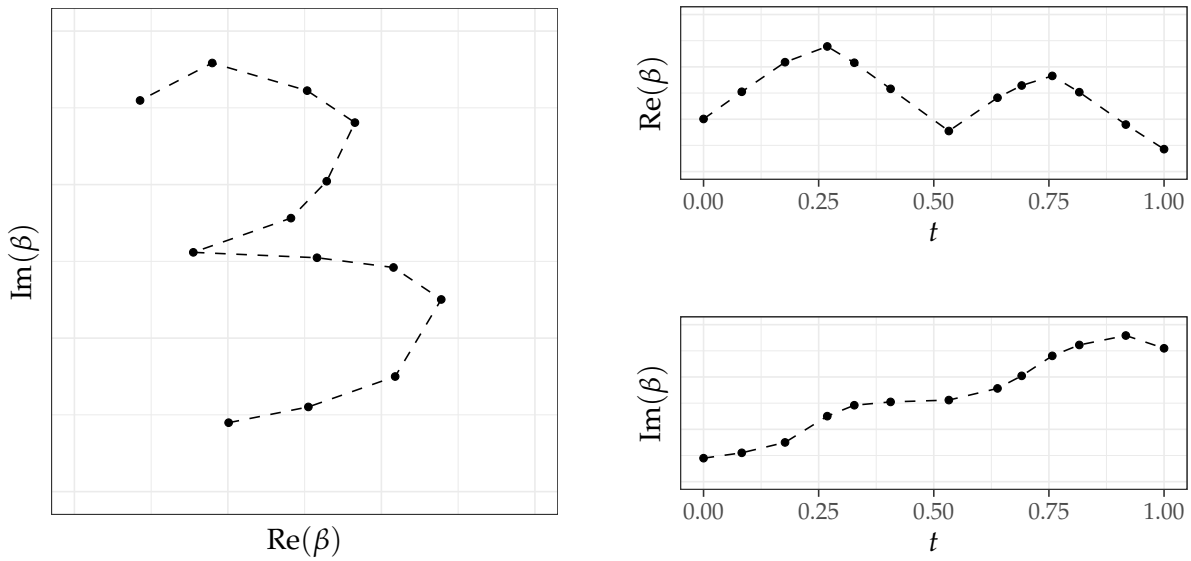

Figure 3.1.: Example of a sparse and irregularly observed digit '3'. Data: `digits3.dat`.

Greven 2021, we may treat a discretely observed curve β as piecewise linear between its observed corners $\beta(t_1), \ldots, \beta(t_n)$, which allows us to calculate a piecewise constant derivative on the intervalls $[t_j, t_{j+1}]$ for $j = 1, \ldots, n-1$. As usually only the image $\beta(t_1), \ldots, \beta(t_n)$ but not the parametrisation $t_1, \ldots, t_n$ is observed, it is first necessary to construct an initial parameterisation. A common choice is an *arc-length-parametrisation*, where we set $t_j = l_j/l$ with $l_j = \sum_{k=1}^{j-1} |\beta(t_{k+1}) - \beta(t_k)|$ the polygon-length up to point j for $j \leq 2$ with $l_1 = 0$ and $l = l_n$.

Consider the piecewise-constant derivative $\Delta\beta\big|_{[t_j,t_{j+1}]} = \frac{\beta(t_{j+1})-\beta(t_j)}{t_{j+1}-t_j}$, which assumes that β is linear between its observed corners. The corresponding SRV curve q can then similarly be treated as piecewise constant $q\big|_{[t_j,t_{j+1}]} = q_j$ with

$$q_j = \Delta\beta\big|_{[t_j,t_{j+1}]} \Big/ \sqrt{\|\Delta\beta\big|_{[t_j,t_{j+1}]}\|} = \frac{\beta(t_{j+1}) - \beta(t_j)}{\sqrt{t_{j+1} - t_j} \cdot \sqrt{\|\beta(t_{j+1}) - \beta(t_j)\|}} \tag{3.1}$$

the constant *square-root-velocity* of β between its corners $\beta(t_j)$ and $\beta(t_{j+1})$. As shown in Steyer, Stöcker, and Greven 2021, Fig. 3, treating the SRV curves as piecewise-constant functions can lead to overfitting, where the mean shape is estimated too polygon-like. As an alternative they propose to approximate the derivative, by assuming that it attains the value of the piecwise-constant derivative $\Delta\beta\big|_{[t_j,t_{j+1}]}$ at the center $s_j = \frac{t_{j+1}-t_j}{2}$ of the interval $[t_j, t_{j+1}]$. Here, this will be used for approximating observa-

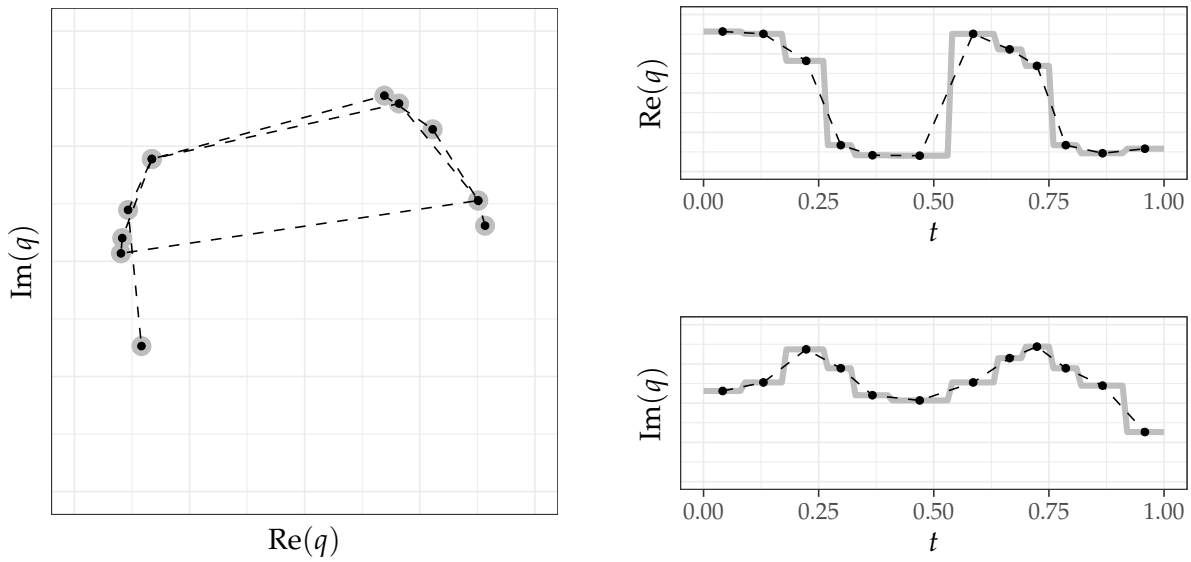

Figure 3.2.: Discretely approximated (black, dashed) and piecewise constant (gray) SRV curve of the digit '3' in Fig. 3.1. Data: `digits3.dat`.

tions $q(s_j) \approx q_j$ of the SRV curve q in the covariance estimation step. See Fig. 3.2 for a visualization of both approaches. Finally, we can approximate the normalized SRV curve $\widetilde{q} = q/\|q\|$ using the polygon-length l of β by $\widetilde{q}_j = q_j/\sqrt{l}$ (see Eq. (2.5)). When considering the warped normalized SRV curve $(q \circ \gamma)\sqrt{\dot{\gamma}}$, the warped discrete derivative is given by $\Delta(\beta \circ \gamma)\big|_{[\gamma^{-1}(t_j),\gamma^{-1}(t_{j+1})]} = \frac{\beta(t_{j+1})-\beta(t_j)}{\gamma^{-1}(t_{j+1})-\gamma^{-1}(t_j)}$. The corresponding warped SRV curve is then given by $(q \circ \gamma)\sqrt{\dot{\gamma}}\big|_{[\gamma^{-1}(t_j),\gamma^{-1}(t_{j+1})]} = \frac{1}{\sqrt{\gamma^{-1}(t_{j+1})-\gamma^{-1}(t_j)}} \cdot \frac{\beta(t_{j+1})-\beta(t_j)}{\sqrt{\|\beta(t_{j+1})-\beta(t_j)\|}}$ (see Steyer, Stöcker, and Greven 2021). Note that this does not change the normalization as re-parametrization is norm-preserving on SRV level.

Discuss normalization?

3.2. Efficient Estimation using Hermitian Covariance Smoothing

Given approximate observations of the warped normalized SRV curves $\widetilde{q}_i^{(k)}(s_{ij})$ for $j = 1, \ldots, n_i - 1$ and $i = 1, \ldots, N$, where n_i denotes the number of observed points per curve, we want to estimate the warping aligned complex covariance surface $C^{(k)}(s,t) = \mathbb{E}[\widetilde{q}^{(k)}(s)\overline{\widetilde{q}^{(k)}(t)}]$. We can treat this estimation as a smoothing problem, by constructing responses $y_{ilm}^{(k)} = \widetilde{q}_i^{(k)}(s_{il})\overline{\widetilde{q}_i^{(k)}(s_{im})}$ and treating the pairs s_{il}, s_{im} as covariates s and t. Smoothing the responses $y_{ilm}^{(k)}$ gives an estimate $\hat{C}^{(k)}(s,t)$ of $C^{(k)}(s,t)$, as each response has expectation $\mathbb{E}[y_{ilm}^{(k)}|s_{il}, s_{im}] = C^{(k)}(s_{il}, s_{im})$. We carry out the

Cov smoothing citations

smoothing in a flexible *penalized tensor product spline* basis

$$C^{(k)}(s,t) = b(s)^\top \Xi^{(k)} b(t) \tag{3.2}$$

where $b(s) = (b_1(s), \ldots, b_K(s))$ denotes the vector of a spline basis and $\Xi^{(k)}$ is a $K \times K$ coefficient matrix to be estimated under a roughness penalty to prevent overfitting. As $C^{(k)}(s,t)$ is complex, we choose the spline basis to be real-valued with $b_j : [0,1] \to \mathbb{R}$ for $j = 1, \ldots, K$ and the coefficient matrix to be complex-valued with $\Xi^{(k)} \in \mathbb{C}^{K \times K}$ without loss of generality. The exact choice of basis and penalty will be discussed in Section 3.3.

Taking into account the symmetry properties of the covariance surface by considering every unique pair (s_{il}, s_{im}) only once allows for more efficient estimation, as shown in Cederbaum, Scheipl, and Greven 2018. In the complex case the covariance surface is Hermitian with $C^{(k)}(s,t) = \overline{C^{(k)}(t,s)}$, which means we can decompose the estimation into two seperate regression problems over the symmetric real and skew-symmetric imaginary parts of $C^{(k)}(s,t)$. We estimate the two models

Formal ok?

$$\mathbb{E}[\mathrm{Re}(y^{(k)})|s,t] = b(s)^\top \Xi^{(k)}_{\mathrm{Re}} b(t) \tag{3.3}$$

$$\mathbb{E}[\mathrm{Im}(y^{(k)})|s,t] = b(s)^\top \Xi^{(k)}_{\mathrm{Im}} b(t)\,, \tag{3.4}$$

with $\Xi^{(k)}_{\mathrm{Re}}, \Xi^{(k)}_{\mathrm{Im}} \in \mathbb{R}^{K \times K}$ and $\Xi^{(k)} = \Xi^{(k)}_{\mathrm{Re}} + \mathrm{i}\Xi^{(k)}_{\mathrm{Im}}$, under the constraints that $(\Xi^{(k)}_{\mathrm{Re}})^\top = \Xi^{(k)}_{\mathrm{Re}}$ and $(\Xi^{(k)}_{\mathrm{Im}})^\top = -\Xi^{(k)}_{\mathrm{Im}}$.

In this thesis $\Xi^{(k)}_{\mathrm{Re}}$ and $\Xi^{(k)}_{\mathrm{Im}}$ are estimated using the `gam` function from the `R` package `mgcv` (Wood 2017), where the smoothing parameters are selected via restricted maximum likelihood (REML) estimation. Two `mgcv` smooths provided in the package `sparseFLMM` (Cederbaum, Volkmann, and Stöcker 2021) are used for efficient Hermitian smoothing, which generalize the approach proposed by Cederbaum, Scheipl, and Greven 2018 for symmetric tensor product P-splines to the skew-symmetric case. Note that `mgcv` automatically adds a sum-to-zero constraint to a specified basis (see Wood 2017, p. 175), which makes it is necessary to transform the coefficient matrices $\widetilde{\Xi}^{(k)}_{\mathrm{Re}}, \widetilde{\Xi}^{(k)}_{\mathrm{Im}}$ recovered from `gam` with an appropriate transformation matrix D. The coefficient matrices in the specified basis are given by $\Xi^{(k)}_{\mathrm{Re/Im}} = D \cdot \widetilde{\Xi}^{(k)}_{\mathrm{Re/Im}}$, where D may be calculated from the constrained and unconstrained design matrices via

$X = D \cdot \widetilde{X}$.

3.3. Estimating the Elastic Full Procrustes Mean in a Fixed Basis

Our goal is to estimate a smooth mean function, which might be constructed with the same univariate basis $b(s)$ used in the tensor product basis of the covariance surface, so that the mean is given by $\mu_q(s) = b(s)^\top \theta$. We can choose an appropriate basis $b(s)$ by considering which, e.g., smoothness properties we want the estimated mean to have. In this thesis we will use penalized B-spline basis functions (P-splines), which are piecewise polynomials of degree l, fused at m knots $\{\kappa_j\}_{j=1,\dots,m}$, where the p-th order differences between coefficients of neighbouring splines are penalized in the covariance estimation (see Fahrmeier et al. 2013, Chap. 8.1). It shold be noted that by using a penalty, the number and location of knots do not have an influence on the estimated function when their number is high enough and they are evenly distributed. Furthermore, because of results relating to the identifiability of spline SRV curves modulo warping and translation, only piecewise linear ($l = 1$) and piecewise constant ($l = 0$) B-splines will be considered in the estimation (see Steyer, Stöcker, and Greven 2021). See Fig. 3.3 for examples of a covariance surface estimated using piecewise constant and piecewise linear P-splines. This still provides the flexibility of estimating either polygonal or smooth means, as the mean function on original curve level is calculated by integration (see Fig. 3.4).

To calculate the elastic full Procrustes Mean, a functional eigenvalue problem on the estimated covariance surface $\hat{C}(s,t) = b(s)^\top \hat{\Xi} b(t)$ had to be solved (omitting '$\cdot^{(k)}$' in this section). Remember that the elastic full Procrustes mean (for fixed warping) is estimated by the solution to the optimization problem

$$\hat{\mu}_q = \underset{\mu_q \in \mathbb{L}^2,\, \|\mu_q\|=1}{\operatorname{argmax}} \int_0^1 \int_0^1 \overline{\mu_q(s)} \hat{C}(s,t) \mu_q(t) \, \mathrm{d}s \, \mathrm{d}t \ . \tag{3.5}$$

Then, estimating the mean $\hat{\mu}_q(s) = b(s)^\top \theta$ reduces to estimating the vector of coefficients $\theta = (\theta_1, \dots, \theta_K) \in \mathbb{C}^K$ with

$$\hat{\theta} = \underset{\theta \in \mathbb{C}^K,\, \|b^\top \theta\|=1}{\operatorname{argmax}} \int_0^1 \int_0^1 \theta^H b(s) b(s)^\top \hat{\Xi} b(t) b(t)^\top \theta \, \mathrm{d}s \, \mathrm{d}t \tag{3.6}$$

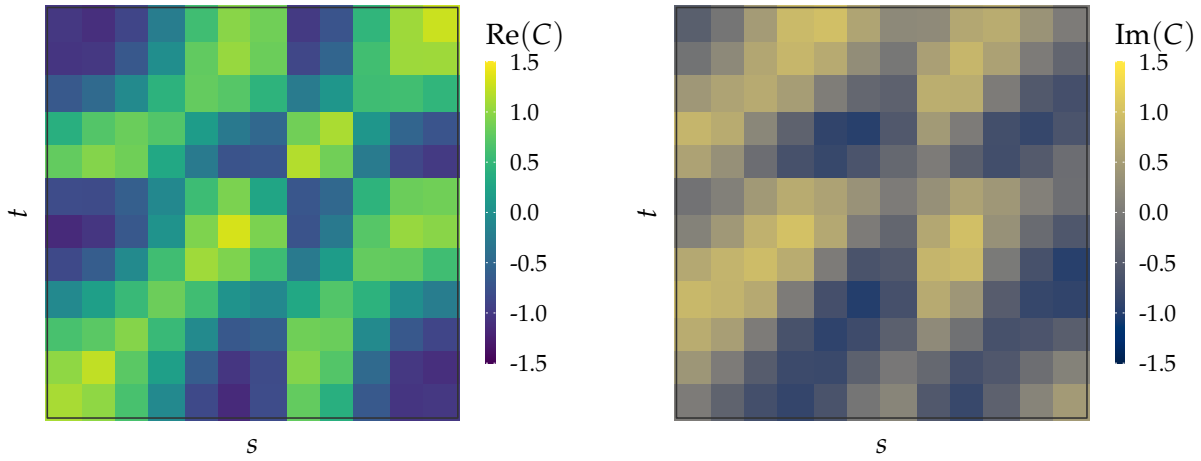

(a) Symmetric real part ($l = 0$)

(b) Skew-symmetric imaginary part ($l = 0$)

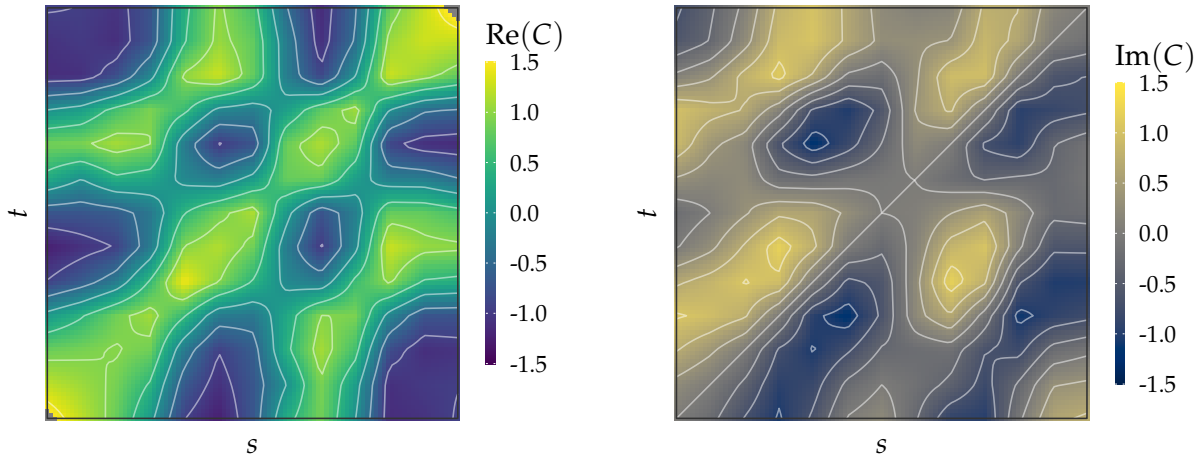

(c) Symmetric real part ($l = 1$)

(d) Skew-symmetric imaginary part ($l = 1$)

Figure 3.3.: Complex covariance surface on SRV curve level. Estimated using 13 equidistant knots, a 2nd order penalty and piecewise constant (top) or piecewise linear (bottom) B-splines. Data: `digits3.dat`

$$= \underset{\theta \in \mathbb{C}^K, \|b^\top \theta\| = 1}{\operatorname{argmax}} \theta^H \left(\int_0^1 b(s) b(s)^\top \, \mathrm{d}s \right) \hat{\Xi} \left(\int_0^1 b(t) b(t)^\top \, \mathrm{d}t \right) \theta \tag{3.7}$$

$$= \underset{\theta \in \mathbb{C}^K, \theta^H G \theta = 1}{\operatorname{argmax}} \theta^H G \hat{\Xi} G \theta \tag{3.8}$$

where $(\cdot)^H = \overline{(\cdot)}^\top$ denotes the conjugate transpose and G is the $K \times K$ Gram matrix with entries given by the basis products $g_{ij} = \langle b_i, b_j \rangle$. For an orthonormal basis the Gram matrix is an identity matrix as $\langle b_i, b_j \rangle = \delta_{ij}$, however, this is not the case for many basis representations such as, e.g.,the B-spline basis. In thesis the `R` package `orthogonalsplinebasis` (Redd 2015) is used to calculate Gram matrices for B-splines analytically, using the methods laid out in Redd 2012.

Having reduced the functional eigenvalue problem to a multivariate eigenvalue problem over the covariance coefficient matrix, we may solve it using Lagrange optimization with the following Langrangian:

$$\mathcal{L}(\theta, \lambda) = \theta^H G \hat{\Xi} G \theta - \lambda(\theta^H G \theta - 1) \tag{3.9}$$

Taking into account that we identified $\mathbb{R}^2$ with $\mathbb{C}$ we can split everything into real and imaginary parts and optimize with respect to $\mathrm{Re}(\theta)$ and $\mathrm{Im}(\theta)$ seperately, which avoids having to take complex derivatives. Using $\theta = \theta_{\mathrm{Re}} + \mathrm{i}\theta_{\mathrm{Im}}$ and $\hat{\Xi} = \hat{\Xi}_{\mathrm{Re}} + \mathrm{i}\hat{\Xi}_{\mathrm{Im}}$ we can write

$$\begin{aligned}\mathcal{L}(\theta_{\mathrm{Re}}, \theta_{\mathrm{Im}}, \lambda) = (\theta_{\mathrm{Re}}^\top - \mathrm{i}\theta_{\mathrm{Im}}^\top) G (\hat{\Xi}_{\mathrm{Re}} + \mathrm{i}\hat{\Xi}_{\mathrm{Im}}) G (\theta_{\mathrm{Re}} + \mathrm{i}\theta_{\mathrm{Im}}) \\ - \lambda \left((\theta_{\mathrm{Re}}^\top - \mathrm{i}\theta_{\mathrm{Im}}^\top) G (\theta_{\mathrm{Re}} + \mathrm{i}\theta_{\mathrm{Im}}) - 1 \right).\end{aligned}$$

By multiplying everything out and using $\hat{\Xi}_{\mathrm{Re}}^\top = \hat{\Xi}_{\mathrm{Re}}$ and $\hat{\Xi}_{\mathrm{Im}}^\top = -\hat{\Xi}_{\mathrm{Im}}$ we get

$$\begin{aligned}\mathcal{L}(\theta_{\mathrm{Re}}, \theta_{\mathrm{Im}}, \lambda) = \theta_{\mathrm{Re}}^\top G \hat{\Xi}_{\mathrm{Re}} G \theta_{\mathrm{Re}} + \mathrm{i}\theta_{\mathrm{Re}}^\top G \hat{\Xi}_{\mathrm{Im}} G \theta_{\mathrm{Re}} + \theta_{\mathrm{Im}}^\top G \hat{\Xi}_{\mathrm{Im}} G \theta_{\mathrm{Re}} - \theta_{\mathrm{Re}}^\top G \hat{\Xi}_{\mathrm{Im}} G \theta_{\mathrm{Im}} \\ + \theta_{\mathrm{Im}}^\top G \hat{\Xi}_{\mathrm{Re}} G \theta_{\mathrm{Im}} + \mathrm{i}\theta_{\mathrm{Im}}^\top G \hat{\Xi}_{\mathrm{Im}} G \theta_{\mathrm{Im}} + \lambda \theta_{\mathrm{Re}}^\top G \theta_{\mathrm{Re}} + \lambda \theta_{\mathrm{Im}}^\top G \theta_{\mathrm{Im}} - \lambda \,.\end{aligned}$$

Differentiation with respect to θ_{Re} and θ_{Im} yield

$$\frac{\partial \mathcal{L}}{\partial \theta_{\mathrm{Re}}} = 2G\hat{\Xi}_{\mathrm{Re}} G\theta_{\mathrm{Re}} - 2G\hat{\Xi}_{\mathrm{Im}} G\theta_{\mathrm{Im}} - 2\lambda G\theta_{\mathrm{Re}} \stackrel{!}{=} 0 \tag{3.10}$$

$$\frac{\partial \mathcal{L}}{\partial \theta_{\mathrm{Im}}} = 2G\hat{\Xi}_{\mathrm{Re}} G\theta_{\mathrm{Im}} + 2G\hat{\Xi}_{\mathrm{Im}} G\theta_{\mathrm{Re}} - 2\lambda G\theta_{\mathrm{Im}} \stackrel{!}{=} 0 \tag{3.11}$$

with the additional constraint $\theta_{\mathrm{Re}}^\top G\theta_{\mathrm{Re}} + \theta_{\mathrm{Im}}^\top G\theta_{\mathrm{Im}} = 1$. We can simplify this further and multiply Eq. (3.11) by i, leading to

$$\hat{\Xi}_{\mathrm{Re}} G\theta_{\mathrm{Re}} - \hat{\Xi}_{\mathrm{Im}} G\theta_{\mathrm{Im}} = \lambda\theta_{\mathrm{Re}} \tag{3.12}$$

$$\mathrm{i}\hat{\Xi}_{\mathrm{Re}} G\theta_{\mathrm{Im}} + \mathrm{i}\hat{\Xi}_{\mathrm{Im}} G\theta_{\mathrm{Re}} = \mathrm{i}\lambda\theta_{\mathrm{Im}} \,. \tag{3.13}$$

Adding both equations finally leads to

$$(\hat{\Xi}_{\mathrm{Re}} + \mathrm{i}\hat{\Xi}_{\mathrm{Im}}) G(\theta_{\mathrm{Re}} + \mathrm{i}\theta_{\mathrm{Im}}) = \lambda(\theta_{\mathrm{Re}} + \mathrm{i}\theta_{\mathrm{Im}}) \tag{3.14}$$

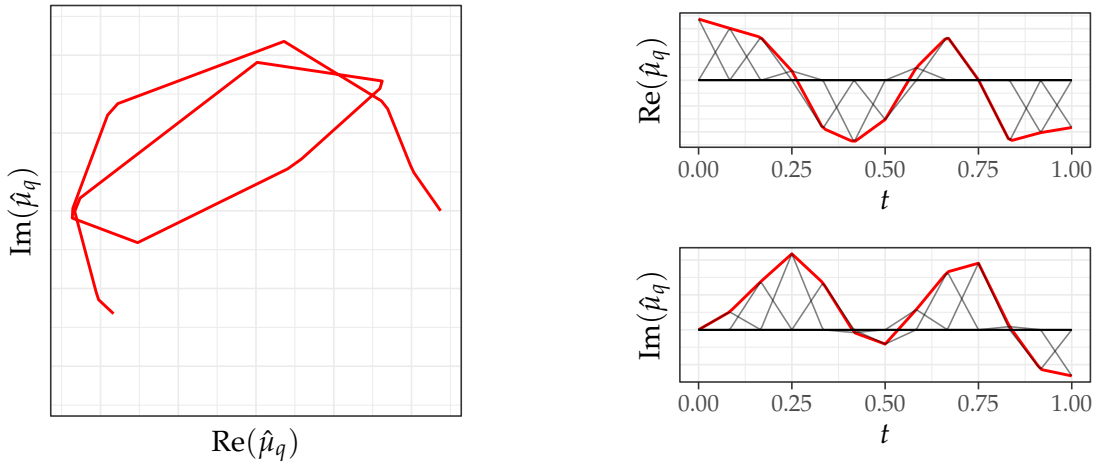

(a) Mean function $\hat{\mu}_q(t) = b(t)^\top \hat{\theta}$ on SRV level with scaled linear B-spline basis functions (right).

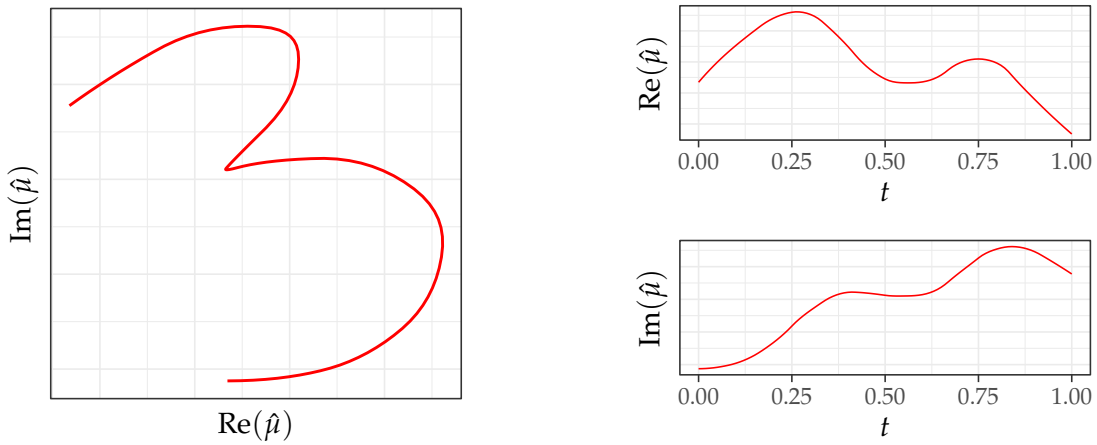

(b) Mean function $\hat{\mu}(t) = \int_0^t \hat{\mu}_q(s)\|\hat{\mu}_q(s)\| \, \mathrm{d}s$ on (unit-length) original curve level.

Figure 3.4.: Elastic full Procrustes mean of handwritten digits '3'. Estimated using 13 equidistant knots, a 2nd order penalty and piecewise linear B-splines. Data: `digits3.dat`

$$\hat{\Xi} G \theta = \lambda \theta \tag{3.15}$$

which is an eigenvalue problem on the product of the complex coefficient matrix and the Gram matrix. Note that this mirrors the result by Reiss and Xu 2020 for FPCA on real-valued tensor product spline coefficient matrices. Multiplying by $\theta^H G$ from the left and using $\theta^H G \theta = 1$ yields $\lambda = \theta^H G \hat{\Xi} G \theta$, i.e. the eigenvalues λ correspond to the target function to maximize (see Eq. (3.8)). It follows that the estimate for the coefficient vector of the elastic full Procrustes mean $\hat{\theta}$ is given by the eigenvector of the leading eigenvalue of $\hat{\Xi} G$ or likewise of $\hat{\Xi}^{(k)} G$, when taking into account the warping alignment in step k of Algorithm 2.2.

3.4. Numerical Integration of the Warping-Aligned Procrustes Fits

Given an estimated mean function $\hat{\mu}_q^{(k)} = b(s)^\top \hat{\theta}^{(k)}$, we need to calculate the Procrustes alignment $\omega_i^{(k)} = \langle \widetilde{q}_i^{(k)}, \hat{\mu}_q^{(k)} \rangle$, $i = 1, \ldots, N$, of each curve onto the current mean, before we can update the warping alignment (see Algorithm 2.2). In the sparse and irregular setting, calculating a scalar product such as $\langle \widetilde{q}_i^{(k)}, \hat{\mu}_q^{(k)} \rangle$ can be a challenge, as we have to evaluate $\widetilde{q}_i^{(k)}(t)$ at every $t \in [0, 1]$.

$$\langle \widetilde{q}_i^{(k)}, \hat{\mu}_q^{(k)} \rangle = \int_0^1 \langle \widetilde{q}_i^{(k)}(t), \hat{\mu}_q^{(k)}(t) \rangle \, \mathrm{d}t \tag{3.16}$$

Following Steyer, Stöcker, and Greven 2021 and as discussed in Section 3.1, this may be approximated by treating $\widetilde{q}_i^{(k)}$ as piecewise constant between the warping-aligned corners of the original curve β_i, with the normalized and warping aligned values given by

$$\widetilde{q}_i^{(k)} \Big|_{\left[\left(\gamma_i^{(k)}\right)^{-1}(t_{ij}), \left(\gamma_i^{(k)}\right)^{-1}(t_{ij+1})\right]} = \widetilde{q}_{ij}^{(k)} \tag{3.17}$$

with $j = 1, \ldots, m_i - 1$ for m_i the number of observed points of the original curve β_i and where

$$\widetilde{q}_{ij}^{(k)} = \frac{1}{\sqrt{L[\beta_i]}} \cdot \frac{1}{\sqrt{\left(\gamma_i^{(k)}\right)^{-1}(t_{ij+1}) - \left(\gamma_i^{(k)}\right)^{-1}(t_{ij})}} \cdot \frac{\beta_i(t_{ij+1}) - \beta_i(t_{ij})}{\sqrt{\|\beta_i(t_{ij+1}) - \beta_i(t_{ij})\|}}. \tag{3.18}$$

Given a fully observed smooth mean function $\hat{\mu}_q^{(k)}$ we can then analytically calculate the scalar product as

$$\langle \widetilde{q}_i^{(k)}, \hat{\mu}_q^{(k)} \rangle = \int_0^1 \langle \widetilde{q}_i^{(k)}(t), \hat{\mu}_q^{(k)}(t) \rangle \, \mathrm{d}t = \sum_{j=0}^{m_i - 1} \int_{\left(\gamma_i^{(k)}\right)^{-1}(t_{ij})}^{\left(\gamma_i^{(k)}\right)^{-1}(t_{ij+1})} \langle \widetilde{q}_{ij}^{(k)}, \hat{\mu}_q^{(k)}(t) \rangle \, \mathrm{d}t \, . \tag{3.19}$$

Noch ein paragraph zu curve-wise interplation mit der penalty auf cov matrix. Verweis auf appendix.

4. Verification and Application using Simulated and Empirical Datasets

In this chapter the proposed methods will be applied and verified. Section 4.1 offers a comparison between the elastic full Procrustes mean, the elastic mean and the full Procrustes mean over two datasets, with the goal of illustrating some properties of the elastic full Procrustes mean. Section 4.2 will briefly discuss the effect of the penalty parameter on the estimation. Section 4.3 discusses .... Finally, Section 4.4 applies the proposed methods to an empirical dataset of tounge shapes, which was kindly provided by ....

Anpassen

Phonetics Data Citations

4.1. Comparison to the Elastic and the Full Procrustes Mean

In this section we will estimate and compare the elastic mean, the full Procrustes mean and the elastic full Procrustes mean for two datasets. The first dataset is the `digits3.dat` dataset provided in the `shapes` package (Dryden 2019) and originally collected by Anderson 1997, which has already been used throughout this thesis for illustrative purposes. It consist of 30 handwritten digits '3', each of which was sampled in a regular fashion at 13 points along the digit, leading to sparse but somewhat regular observations. The second dataset consists of ten simulated spirals, each of which is a sample of the curve $\beta(t) = t\cos(13t) + \mathrm{i} \cdot t\sin(13t)$, evaluated $m_i \in [10, 15]$ times over a noisy grid, with additional noise applied to the output, leading to sparse and irregular observations. The code simulating these spirals was adapted from the `compute_elastic_mean` function's documenation in the `elasdics` package (Steyer 2021). Because the spirals "speed up" w.r.t. t towards the end ($t = 1$), they start out quite densly sampled but become increasingly sparser, making the mean estimation, especially close to $t = 1$, a challenge. The datasets are considered in two settings: In the first, each dataset is considered as is, which means that all curves are centered and similarly aligned. In the second, for each curve β_i a random Euclidean similarity

transform with translation $\xi_i \sim \mathcal{U}([\xi_{\min}, \xi_{\max}])$, rotation $\theta_i \sim \mathcal{U}([0, 2\pi))$ and scaling $\lambda_i \sim \mathcal{U}([0.5, 1.5])$ is drawn, where $\xi_{\min}, \xi_{\max}$ are set respectively to ± 60 and ± 2 for the digits and spirals. The curves are then transformed by $\lambda_i e^{i\theta_i} \beta_i + \xi_i$.

The four sets of data curves and means, are show in Fig. 4.1. Here, the elastic mean (blue) is estimated using `compute_elastic_mean` from the `elasdics` package. The full Procrustes (green) and the elastic full Procrustes mean (red) are estimated using the methods proposed in Chapters 2 and 3, where for the full Procrustes mean the estimation is stopped before the warping alignment step during the first iteration. Note that the full Procrustes mean calculated in this way is not exactly a minimizer of the sum of squared full Procrustes distance defined in Definition 2.2, but instead is a minimizer of the sum of squared full Procrustes distances on SRV level. When comparing the different mean types in Fig. 4.1 we can see that, unlike the elastic mean, both Procrustes means are invariant with respect to all Euclidean similarity transforms, as the estimated mean is the same for the transformed and original datasets. However for this very same reason, both Procrustes means hold no information about the scale or rotation of the original curves, as they are of unit-length and have a rotation dependent on the eigendecomposition of the covariance surface. The elastic mean is invariant only with respect to re-parametrization and translation, so that its scale and rotation match the original data curves. It can therefore be meaningfully plotted together with the original curves, when they are centered.

Vielleicht sogar doch "exactly?"

Apart from illustrating these properties, Fig. 4.1 provides two important validation checks for the estimation procedure proposed in Chapters 2 and 3. Firstly, as stated, the estimated elastic full Procrustes mean is invariant to all Euclidean similarity transforms, as the mean shapes do not change with transformations of the input curves. Secondly, when considering untransformed curves, the estimated elastic full Procrustes mean shapes are very compareable to elastic mean shapes estimated with the method proposed in Steyer, Stöcker, and Greven 2021. This is especially noteable when comparing the means in Fig. 4.1 (a) where the prominent “notch” in the center of the mean shape is similarly pronounced for the elastic and the elastic full Procrustes means, but not for the (non-elastic) full Procrustes mean. Taken together this shows that the proposed mean estimation method provides elastic mean estimates in the setting of sparse and irregular curves, which are invariant to all shape-preserving

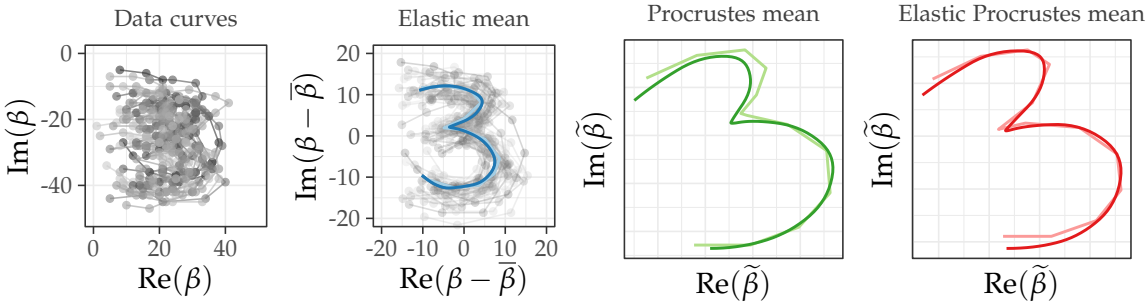

(a) Means for `digits3.dat`.

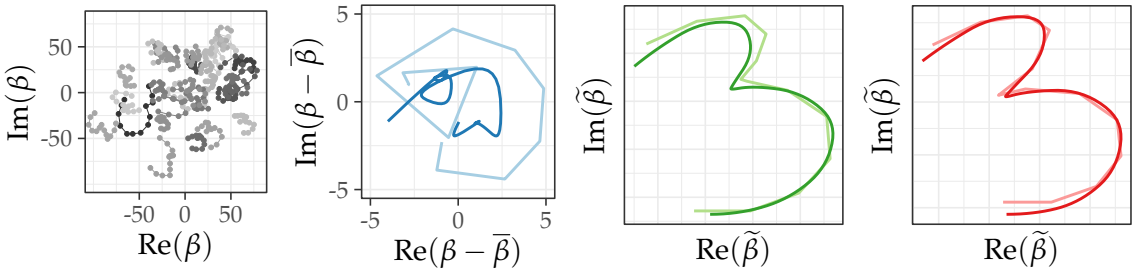

(b) Means for `digits3.dat` with random Euclidean similarity transform applied.

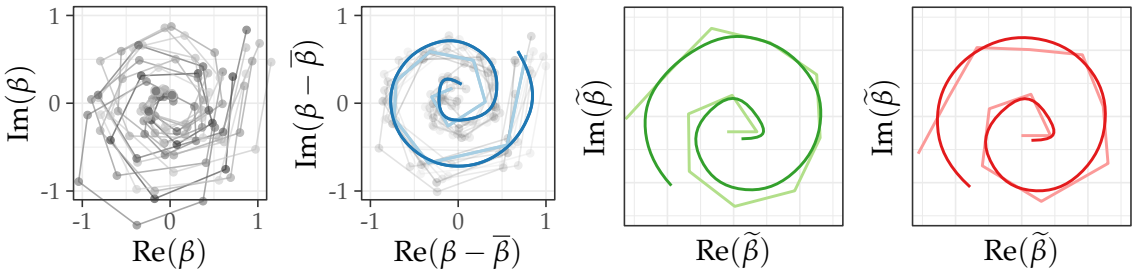

(c) Means for simulated sparse spirals.

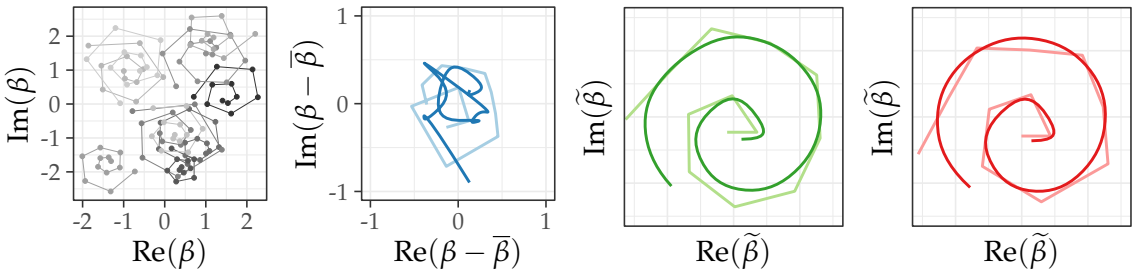

(d) Means for simulated sparse spirals with random Euclidean similarity transform applied.

Figure 4.1.: Comparison of three mean types: Elastic mean (blue), full Procrustes mean (green) and elastic full Procrustes mean (red), estimated over four sets of data curves (grey). Each mean is estimated as polygonal (light, 16 knots) and smooth (dark, 13 knots), where in the estimation of the two Procrustes means a 2nd order penalty was applied. Data: See Section 4.1

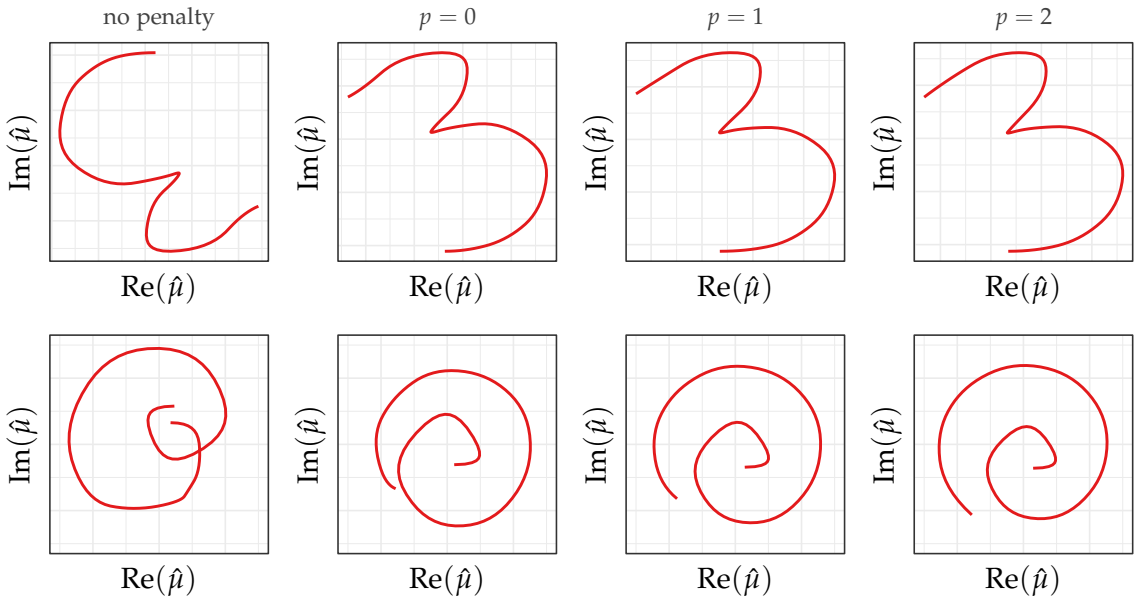

Figure 4.2.: Elastic full Procrustes mean under different penalties. Estimated using no penalty (left) and order 0/1/2 penalties (center-left/center-right/right) respectively, as well as 13 equidistant knots and linear B-splines on SRV level. Data: See Figs. 4.1b and 4.1d

transformations.

4.2. Effect of the Penalty on the Estimated Mean

The elastic full Procrustes mean is given by the leading eigenfunction of the complex covariance surface, which was estimated using tensor product P-splines. As a consequence, the order of the roughness penalty applied in the estimation of the covariance surface directly influences the shape of the estimated mean function. This can be seen in Fig. 4.2, where a smooth mean was estimated for different penalties. Here, in particular, the spiral mean shapes help to illustrate the penalty effect. As mentioned in Section 4.1, the spirals are evaluated in a way that makes them very sparse towards the end, leading to unstable mean estimates in that region. By penalizing p-th order differences between neighbouring coefficients, the penalty helps to stabilize the covariance estimation (and thereby the mean) in regions where observations are sparse, where the shape of the function is consequently dominated by the penalty.

The mean function on the far left in Fig. 4.2 was estimated using no penalty. We can see that the spiral shape is estimated well in the beginning (central part), where observations are dense, but becomes increasingly unstable and wriggly towards the

end (outer part). The mean function on the center-left was estimated using a zero order penalty. A zero order penalty on a B-spline basis can be interpreted as a ridge-penalty on the basis coefficients, i.e. the basis coefficients (and therefore the estimated function) get shrinked towards zero in areas where observations are sparse. It is important to note that the penalized covariance estimation is performed on SRV level and not on data curve level, which means the ridge penalty shrinks the estimated SRV mean towards zero. However, this does not imply that the estimated mean on data curve level also gets shrunk towards zero. In fact, a ridge penalty on SRV level only shrinks the *absolute velocity* of the mean on data curve level towards zero, but should not directly influence the *direction* of the mean curve. This can be seen, when comparing the zero order penalty spiral mean (center-left) to the higher order penalty spiral means (right) and noting that, as a consequence of the decreased absolute velocity, it is relatively "shorter" towards the end when compared to the beginning of the spiral. The higher order penalties may be interpreted as smoothing the SRV mean function towards a polynomal of degree $p-1$ in areas where the penalty dominates, which means a constant function for the first order penalty and a linear function for the second order penalty (see e.g. Fahrmeier et al. 2013, p. 435). Looking at the means for $p = 1, 2$ in Fig. 4.2, these differences are already hard to spot. The order two mean (right) is slightly longer towards the end, indicating a speed up, which is caused by the penalization towards a global linearly (increasing) velocity, compared to a more conservative penalization towards a global constant velocity.

Kann man das so einfach übertrage?

4.3. Elastic Full Procrustes Fits and Outliers

Although the elastic full Procrustes mean does not share rotation, scale and translation as the input curves, it is still possible to visually compare them, by plotting the mean together with the elastic full Procrustes fits. In this thesis, the elastic full Procrustes fits are calculated on SRV level as $\widetilde{q}^{\mathrm{EP}} = (\omega^{\mathrm{opt}} \cdot \widetilde{q} \circ \gamma^{\mathrm{opt}})\sqrt{\dot{\gamma}^{\mathrm{opt}}}$, where the optimal rotation and scaling alignment $\omega^{\mathrm{opt}} = \lambda^{\mathrm{opt}} e^{\mathrm{i}\theta^{\mathrm{opt}}}$ and optimal warping alignment γ^{opt} of each curve to the mean are taken from the last iteration of the mean estimation step. In Fig. 4.3 the elastic full Procrustes mean and fits are plotted for the digits '3' and simulated spiral datasets discussed in Section 4.1, whith a random Euclidean similarity transform was applied to each curve. This alignment works very well for the simluated

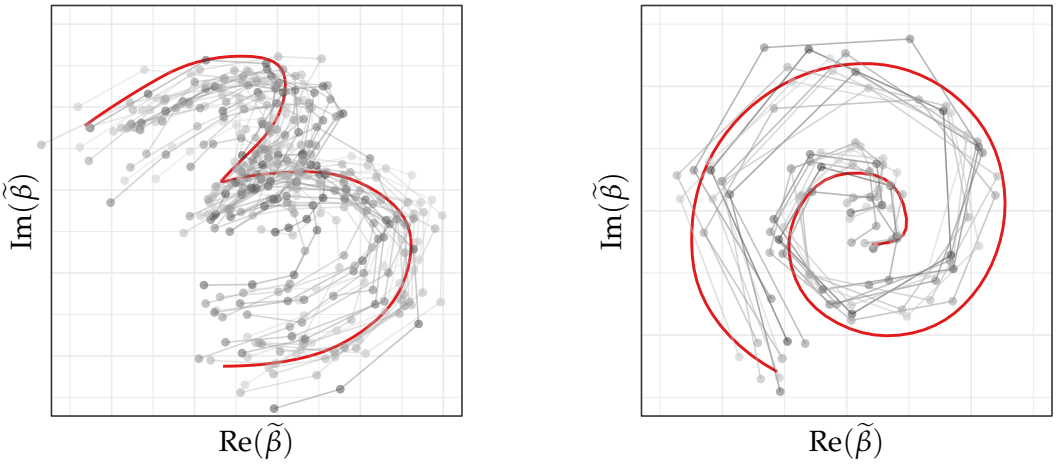

Figure 4.3.: Centered elastic full Procrustes fits (grey) and smooth means (red). Parameters: Second order penalty and linear B-splines, with 13 (left) and 19 (right) equidistant knots. Data: See Figs. 4.1b and 4.1d

spirals and is more fuzzy for the digits, due to their greater variability in shape.

In general, one has to be careful when interpreting these plots. For example, it can be seen that the estimated mean does not necessarily follow the "center of mass" of the aligned curves. One reason for this is that the mean is calculated on SRV level, meaning we may set an arbitrary translation for the mean on data curve level. Here, the Procrustes fits and the mean function are centered, but a natural alternative might be to have all curves start at the origin, with both choices leading to very different, but equally valid, visual representations. It should also be taken into account that the mean is calculated from a smooth covariance surface, which was estimated using a roughness penalty (see Section 3.2), while the optimal rotation and scaling alignment was calculated by an approximation, where the observed normalized SRV curves are assumed piecewise-constant (see Section 3.4).

See Figure Fig. 4.4. ... See also Appendix A.3.

Outlier diskutieren

4.4. Variability in Tounge Shapes in a Phonetics Dataset

[Paragraph: Einleitung, Ultraschallaufnahmen, Zungendaten]

[Paragraph: Datensatz, (r, θ) zu (x_1, x_2), Arten der Varibilität $\rightarrow$ Wörter + Versuchspersonen + Wiederholungen]

[Paragraph: Fragestellung, Variabilität über Vokalkontext (quasi Wiederholung der Untersuchung aus dem Consulting Projekt)]

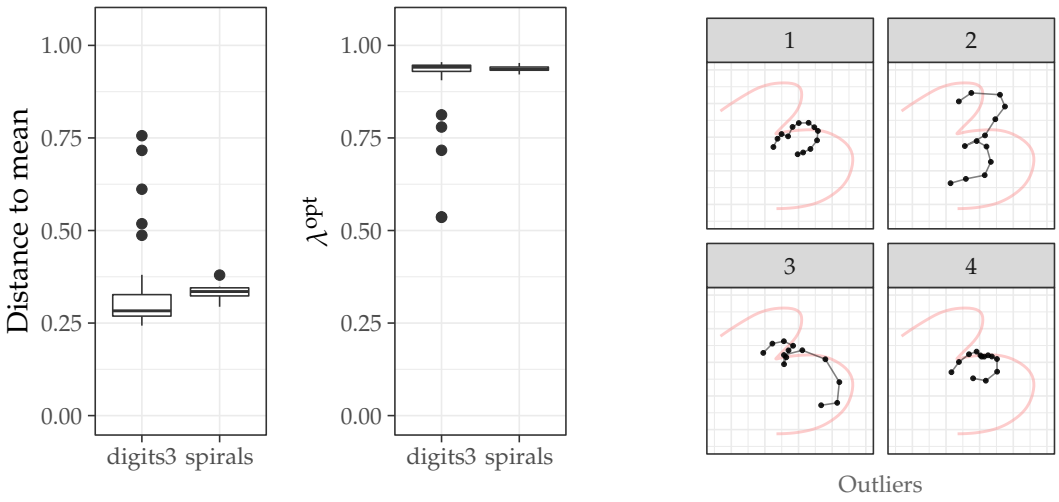

Figure 4.4.: Left: Distribution of each curves elastic full Procrustes distance to the estimated mean. Center-left: Distribution of the scaling parameter of each elastic Procrustes fit onto the estimated mean. Right: Four largest outliers (grey) with respect to their distance to the estimated mean (red) for the `digits3.dat` dataset. Parameters: See Fig. 4.3. Data: See Figs. 4.1b and 4.1d

Summary for Almond

- Want investiage how the effect of the flanking vowels 'aa' and 'ii' on tounge shape differs for the consonants 'd', 'l', 'n' and 's', while controlling for variability over six speakers and 5–7 repetitions of the same word per speaker.
- Analysis should be invariant with respect to size, rotation, translation and parametrization of the tounges. This can e.g. account for anatomical differences between speakers, or inaccuracies in the measurement process.
- **Idea:** Estimate a global mean function $q_0(t)$ from all curves and calculate the elastic full Procrustes residuals. They are given by the difference of elastic full Procrustes fits and the mean function on SRV level

$$\hat{r}_i = \left(\omega_i^{\text{opt}} \cdot \widetilde{q}_i \circ \gamma_i^{\text{opt}}\right) \sqrt{\dot{\gamma}_i^{\text{opt}}} - \hat{q}_0 \,.$$

  We can perform analysis over the $\hat{r}_i(t)$.
- A word is a combination of vowels and consonants (C_v, C_c) with $C_v \in \{\text{aa}, \text{ii}\}$ and $C_c \in \{\text{d}, \text{l}, \text{n}, \text{s}\}$, e.g. 'pada' corresponds to (aa, d) as all words start with 'p'. We can index each word–speaker pair (C_v, C_c, C_s) by k, where $C_s \in \{1, \ldots, 6\}$

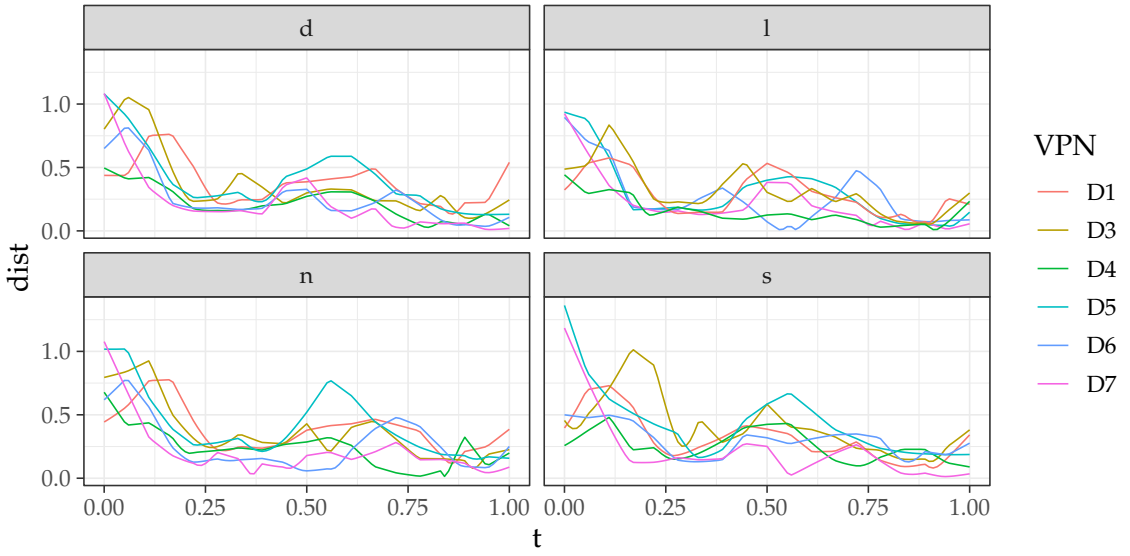

Figure 4.5.: a caption

and $k = 1, \ldots, K$ with $K = 2 \cdot 4 \cdot 6 = 48$.

- Then we can gather the residuals $\hat{r}_{(k,rep_k)}(s_{(k,rep_k,j)})$ of the repetitions rep_k (their number varies with k) of each word–speaker pair k, and estimate a 'mean' residual function for that word and speaker:

$$\hat{r}_k(t) = \hat{r}_{(C_v,C_c,C_s)}(t) \approx \hat{\theta}_k^\top b(t)$$

  Atm I use the mean basis here, which means linear B-Splines. Might be nicer to have something that is smoother.

- We are interested in the effect of the flanking vowels on tounge shape given, for each consonant-speaker pair, by this difference:

$$\hat{d}_{(C_c,C_s)}(t) = \hat{r}_{(\text{aa},C_c,C_s)}(t) - \hat{r}_{(\text{ii},C_c,C_s)}(t) = \left(\hat{\theta}^\top_{(\text{aa},C_c,C_s)} - \hat{\theta}^\top_{(\text{aa},C_c,C_s)}\right) b(t)\,.$$

  Note that $\hat{d}(t) : [0,1] \to \mathbb{C}$ (two-dimensional)! The absolute differences over speakers and consonants are given by $|\hat{d}_{(C_c,C_s)}(t)|$ are plotted in Fig. 4.5.

- Finally we can average the differences over each speaker as

$$\hat{d}_{(C_c)}(t) = \left(\frac{1}{6}\sum_{C_s} \hat{\theta}^\top_{(C_c,C_s)}\right) b(t)$$

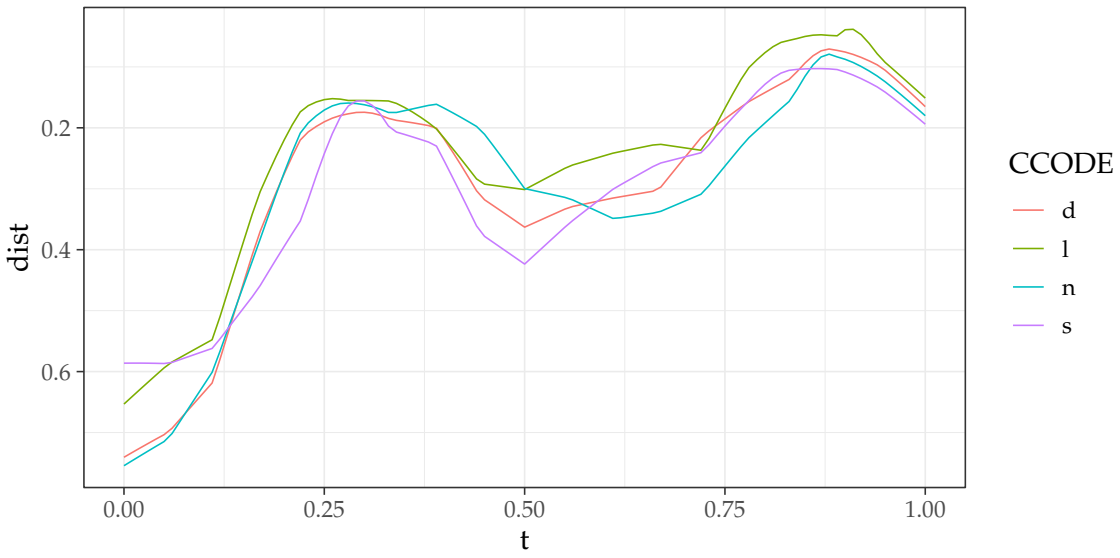

Figure 4.6.: Another caption

or likewise as absolute difference $|\hat{d}_{(C_c)}(t)|$ plotted in Fig. 4.6.

- Man sieht, dass der Einfluss des flankierenden Vokals unabhängig vom Konsanten zu sein scheint. Das ist zumindest ein anderes Ergebniss, als in dem Consulting Projekt.
- Die Analysie ist hier auf SRV level.
- Sofern das alles so Sinn macht, könnte man jetzt noch Konfidenzintervalle undsowas dazu berechnen.

5. Summary and Outlook

Summary zum Schluss schreiben

Bibliography

Anderson, C. R. (1997). *Object recognition using statistical shape analysis*. PhD thesis. University of Leeds.

Cederbaum, J., F. Scheipl, and S. Greven (2018). "Fast Symmetric Additive Covariance Smoothing". In: *Computational Statistics & Data Analysis* 120, pp. 25–41.

Cederbaum, J., A. Volkmann, and A. Stöcker (2021). *sparseFLMM: Functional Linear Mixed Models for Irregularly or Sparsely Sampled Data*. R package version 0.4.0. URL: `https://CRAN.R-project.org/package=sparseFLMM`.

Dryden, I. L. (2019). *`shapes` package*. Contributed package, Version 1.2.5. R Foundation for Statistical Computing. Vienna, Austria. URL: `http://www.R-project.org`.

Dryden, I. L. and K. V. Mardia (2016). *Statistical Shape Analysis with Applications in R*. 2nd ed. John Wiley and Sons Ltd.

Fahrmeier, L. et al. (2013). *Regression. Models, Methods and Applications*. Berlin, Heidelberg: Springer.

Fréchet, M. R. (1948). "Les éléments aléatoires de nature quelconque dans un espace distancié". fr. In: *Annales de l'institut Henri Poincaré* 10.4, pp. 215–310.

Karcher, H. (1977). "Riemannian center of mass and mollifier smoothing". In: *Communications on Pure and Applied Mathematics* 30.5, pp. 509–541.

Kendall, D. G. (1977). "The diffusion of shape". In: *Advances in Applied Probability* 9.3, pp. 428–430.

R Core Team (2021). *R: A Language and Environment for Statistical Computing*. R Foundation for Statistical Computing. Vienna, Austria. URL: `https://www.R-project.org/`.

Ramsay, J. and B. W. Silverman (2005). *Functional Data Analysis*. Springer series in statistics.

Rao, C. R. (1945). "Information and accuracy attainable in the estimation of statistical parameters". In: *Bulletin of Calcutta Mathematical Society* 37, pp. 81–91.

Redd, A. (2012). "A comment on the orthogonalization of B-spline basis functions and their derivatives". In: *Stat Comput* 22, pp. 251–257.

– (2015). *orthogonalsplinebasis: Orthogonal B-Spline Basis Functions*. R package version 0.1.6. url: https://CRAN.R-project.org/package=orthogonalsplinebasis.

Reiss, P. T. and Meng Xu (2020). "Tensor product splines and functional principal components". In: *Journal of Statistical Planning and Inference* 208, pp. 1–12.

Srivastava, A. and E. P. Klassen (2016). *Functional and Shape Data Analysis*. New York: Springer.

Srivastava, A., E. P. Klassen, et al. (2011). "Shape Analysis of Elastic Curves in Euclidean Spaces". In: *IEEE Transactions on Pattern Analysis and Machine Intelligence* 33.7, pp. 1415–1428.

Steyer, L. (2021). *elasdics: Elastic Analysis of Sparse, Dense and Irregular Curves*. R package version 0.1.1. url: https://CRAN.R-project.org/package=elasdics.

Steyer, L., A. Stöcker, and S. Greven (2021). *Elastic analysis of irregularly or sparsely sampled curves*. arXiv: 2104.11039 [stat.ME].

Stöcker, A. and S. Greven (2021). *Functional additive regression on shape and form manifolds of planar curves*. arXiv: 2109.02624 [stat.ME].

Wang, J.-L., J.-M. Chiou, and H.-G. Müller (2016). "Functional Data Analysis". In: *Annual Review of Statistics and Its Application* 3.1, pp. 257–295.

Wood, S.N (2017). *Generalized Additive Models: An Introduction with R*. 2nd ed. Chapman and Hall/CRC.

A. Appendix

A.1. Additional Proofs and Derivations

A.1.1. Derivation of Lemma 2.1

$$\begin{aligned} d_{FP}([\beta_1]_{\text{Eucl}}, [\beta_2]_{\text{Eucl}})^2 &= \min_{\omega \in \mathbb{C}} \|\widetilde{\beta}_1 - \omega \widetilde{\beta}_2\|^2 \\ &= \min_{\lambda \in \mathbb{R}^+, \theta \in [0,2\pi)} \|\widetilde{\beta}_1 - \lambda e^{\mathrm{i}\theta} \widetilde{\beta}_2\|^2 \\ &= \min_{\lambda \in \mathbb{R}^+, \theta \in [0,2\pi)} \langle \widetilde{\beta}_1 - \lambda e^{\mathrm{i}\theta} \widetilde{\beta}_2, \widetilde{\beta}_1 - \lambda e^{\mathrm{i}\theta} \widetilde{\beta}_2 \rangle \\ &= \min_{\lambda \in \mathbb{R}^+, \theta \in [0,2\pi)} \|\widetilde{\beta}_1\|^2 + \lambda^2 \|\widetilde{\beta}_2\|^2 - \lambda (e^{\mathrm{i}\theta} \langle \widetilde{\beta}_1, \widetilde{\beta}_2 \rangle + e^{-\mathrm{i}\theta} \langle \widetilde{\beta}_2, \widetilde{\beta}_1 \rangle \end{aligned}$$

Define $\langle \widetilde{\beta}_1, \widetilde{\beta}_2 \rangle = \kappa e^{\mathrm{i}\phi} \in \mathbb{C}$ with $\kappa \in \mathbb{R}^+$, $\phi \in [0, 2\pi)$ and use $\|\widetilde{\beta}_1\| = \|\widetilde{\beta}_2\| = 1$.

$$\begin{aligned} d_{FP}([\beta_1]_{\text{Eucl}}, [\beta_2]_{\text{Eucl}})^2 &= \min_{\lambda \in \mathbb{R}^+, \theta \in [0,2\pi)} 1 + \lambda^2 - \lambda (e^{\mathrm{i}\theta} \kappa e^{\mathrm{i}\phi} + e^{-\mathrm{i}\theta} \kappa e^{-\mathrm{i}\phi}) \\ &= \min_{\lambda \in \mathbb{R}^+, \theta \in [0,2\pi)} 1 + \lambda^2 - \lambda \kappa \left(e^{\mathrm{i}(\theta+\phi)} + e^{-\mathrm{i}(\theta+\phi)} \right) \\ &= \min_{\lambda \in \mathbb{R}^+} 1 + \lambda^2 - \max_{\theta \in [0,2\pi)} 2\lambda\kappa \cos(\theta + \phi) \\ &\overset{\theta^{\text{opt}} = -\phi}{=} \min_{\lambda \in \mathbb{R}^+} 1 + \lambda^2 - 2\lambda\kappa \end{aligned}$$

From $\frac{\partial}{\partial \lambda} \left(1 + \lambda^2 - 2\lambda\kappa\right) = 2\lambda - 2\kappa \overset{!}{=} 0$ it follows that $\lambda^{\text{opt}} = \kappa$.

$$d_{FP}([\beta_1]_{\text{Eucl}}, [\beta_2]_{\text{Eucl}})^2 = \left(1 + \kappa^2 - 2\kappa^2\right) = \left(1 - \kappa^2\right)$$

Lemma 2.1 i.) follows by considering $\kappa^2 = |\langle \widetilde{\beta}_1, \widetilde{\beta}_2 \rangle|^2 = \langle \widetilde{\beta}_1, \widetilde{\beta}_2 \rangle \langle \widetilde{\beta}_2, \widetilde{\beta}_1 \rangle$. Then

$$d_{FP}([\beta_1]_{\text{Eucl}}, [\beta_2]_{\text{Eucl}}) = \sqrt{1 - \langle \widetilde{\beta}_1, \widetilde{\beta}_2 \rangle \langle \widetilde{\beta}_2, \widetilde{\beta}_1 \rangle}\,.$$

Lemma 2.1 ii.) follows by $\omega^{\text{opt}} = \lambda^{\text{opt}} e^{\mathrm{i}\theta^{\text{opt}}} = \kappa e^{-\mathrm{i}\phi} = \overline{\langle \widetilde{\beta}_1, \widetilde{\beta}_2 \rangle} = \langle \widetilde{\beta}_2, \widetilde{\beta}_1 \rangle$.

A.2. Shape-Smoothing Using the Estimated Covariance-Surface

In Form schreiben.

Idea: Smooth q in mean basis $b(t)$, so that $\hat{q}(t) = b(t)^T \hat{\theta}_q$. Then the scalar products simplify to

$$\langle q, \hat{p} \rangle \approx \hat{\theta}_q^H G \hat{\theta}$$

$$\langle q, q \rangle \approx \hat{\theta}_q^H G \hat{\theta}_q$$

As q can be sparse, we may want to use the estimated covariance matrix $\hat{\Xi}$ when estimating θ_q in the form of a Normal prior $\theta_q \sim \mathcal{N}_{\mathbb{C}^k}(0, \hat{\Xi})$ leading to

$$\hat{\theta}_q = (B^T B + \Xi^{-1})^{-1} B^T q$$

or equivalently using eigendecompositon $\Xi = V \Lambda V^{-1}$ with $V^H V = \mathcal{I}$ and $\Lambda = diag(\lambda_1, \ldots, \lambda_k)$

$$\hat{\theta}_q = V(V^H B^T B V + \Lambda^{-1})^{-1} V^H B^T q$$

In general how well this works tends to depend on how close the curve is to the estimated mean.

Maybe using a penalty parameter - controling the strength of the regularization - is also thinkable? Something like this:

$$\hat{\theta}_q(\lambda) = V(V^H B^T B V + \lambda \cdot \Lambda^{-1})^{-1} V^H B^T q$$

Thought: A normal prior is probably not appropriate, because while its true that $\mathbb{E}[\theta] = 0$ (due to rotational symmetry) I would think that in general $\mathbb{E}[\|\theta\|] \neq 0$. A distribution more like a Normal distribution lying on a ring around 0 with radius $r = \|\theta\|$ is probably better? Then estimates wouldn't be pressed to zero so strongly, and instead would be pressed to curve of size equal to the mean.

A.3. Removing the Iteration over Rotation

As suggested to Lisa

B. Implementation Notes

Ein paar Anmerkungen zum Code

Statutory Declaration

I declare that I have not previously submitted the present work for other examinations and that I wrote this work independently. All sources that I have reproduced in either an unaltered or modified form, have been acknowledged as such. I understand that violations of these principles will result in proceedings regarding deception or attempted deception.

Manuel Pfeuffer
Berlin, 12th December, 2021